Deregulated expression of cytokine receptor gene, *CRLF2*, is involved in lymphoid transformation in B cell precursor acute lymphoblastic leukemia

Short Title - Deregulated *CRLF2* expression in BCP-ALL

L J Russell[1,11], M Capasso[2,11], I Vater[3,11], T Akasaka[2], O A Bernard[4], M J Calasanz[5], T Chandrasekaran[2], E Chapiro[4], S Gesk[3], M Griffiths[6], D S Guttery[2], C Haferlach[7], L Harder[3], O Heidenreich[8], J Irving[8], L Kearney[9], F Nguyen Khac[4], L Machado[2], L Minto[8], A Majid[2], A V Moorman[1], H Morrison[1], V Rand[1], J C Strefford[10], C Schwab[1], H Tönnies[3], M J S Dyer[2,12,13], R Siebert[3,12,13], C J Harrison[1,12,13]

[1]Leukaemia Research Cytogenetics Group, Northern Institute for Cancer Research, Newcastle University, UK; [2]MRC Toxicology Unit, Leicester University, UK; [3]Institute of Human Genetics, Christian Albrechts University & University Hospital Schleswig-Holstein, Kiel, Germany; [4]INSERM E210, Hôpital Necker Enfants Malade, Paris, France; [5]Department of Genetics, University of Navarra, Pamplona, Spain.
[6]West Midlands Regional Genetics Laboratory, Birmingham Women's Hospital, Edgbaston, Birmingham, UK; [7]MLL Münchner Leukämielabor GmbH, Munich, Germany
[8]Northern Institute for Cancer Research, Newcastle University, UK; [9]Section of Haemato-Oncology, Institute of Cancer Research, Brookes Lawley Building, Surrey, UK; [10]Cancer Genomics Group, Cancer Sciences Division, University of Southampton, UK

[11]these authors contributed equally to this work
[12]these authors share senior authorship
[13]correspondence to:
Professor C.J. Harrison, Leukaemia Research Cytogenetics Group, Northern Institute for Cancer Research, Newcastle University, Level 5 Sir James Spence Institute, Royal Victoria Infirmary, Newcastle-upon-Tyne, NE1 4LP UK. Email: christine.harrison@newcastle.ac.uk

Prof. Dr. med. Reiner Siebert, Institute of Human Genetics, University Hospital Schleswig-Holstein Campus, Kiel Schwanenweg 24 D-24105 Kiel, Germany. email: rsiebert@medgen.uni-kiel.de
Professor Martin J.S. MRC Toxicology Unit, Hodgkin Building Room 402, Lancaster Road, Leicester LE1 9HN mjsd1@le.ac.uk

Abstract word count – 179
Main text word count – 4937
Figures – 4
Tables – 1
Supplementary tables – 4
Supplementary figures - 1
References - 34

Appropriate scientific category – Lymphoid neoplasia

Abstract

We report two novel, cryptic chromosomal abnormalities in precursor B-cell acute lymphoblastic leukemia (BCP-ALL): a translocation, either t(X;14)(p22;q32) or t(Y;14)(p11;q32), in 33 patients and an interstitial deletion, either del(X)(p22.33p22.33) or del(Y)(p11.32p11.32), in 64 patients, involving the pseudoautosomal region (PAR1) of the sex chromosomes. The incidence of these abnormalities was 5% in childhood ALL (0.8% with the translocation, 4.2% with the deletion). Patients with the translocation were older (median age 16 years), whilst the patients with the deletion were younger (median age 4 years). The two abnormalities result in deregulated expression of the cytokine receptor, *cytokine receptor-like factor 2*, *CRLF2* (also known as *thymic stromal-derived lymphopoietin receptor*, TSLPR). Over-expression of CRLF2 was associated with activation of the JAK-STAT pathway in cell lines and transduced primary B-cell progenitors, sustaining their proliferation and indicating a causal role of CRLF2 over-expression in lymphoid transformation. In Down Syndrome (DS) ALL and two non DS BCP-ALL cell lines, CRLF2 deregulation was associated with mutations of the *JAK2* pseudokinase domain suggesting oncogenic cooperation, as well as highlighting a link between non DS ALL and *JAK2* mutations.

Introduction

Cytokines and their receptors play an important role in cell survival, proliferation and differentiation during hematopoieis[1]. Cytokine receptors lack intrinsic catalytic activity and depend on the tyrosine kinase (TK) activity of the Janus family of TK. The role of the cytokine *interleukin-7* (IL7) signaling in human lymphoid differentiation differs from its role in mice, but has been extensively demonstrated through the study of naturally occurring mutants[2]. The receptor for IL7 is composed of two chains, *Interleukin-2 receptor gamma* (*IL2RG*) and IL7 receptor alpha (*IL7RA*)[3]. Intracellular signaling from the IL7 receptor is believed to occur through the JAK1 and JAK3 kinases, resulting in activation of the STAT transcription factors.

Thymic stromal-derived lymphopoietin (TSLP) is an epithelial derived cytokine that strongly activates dendritic cells. One significant role of TSLP deregulation is the control of inflammatory and allergic processes[4]. It was isolated as a cytokine mediating B-cell precursor proliferation and survival *in vitro*[5]. The TSLP and IL7 receptors share *IL7RA*, while TSLP possesses an *IL2RG* related second chain: *cytokine receptor-like factor 2* (*CRLF2*) or *TSLPR*. Although signaling from the TSLP receptor is known to lead to STAT5 activation, the precise kinase responsible for this is species specific and remains controversial[6-9].

Acute lymphoblastic leukemia (ALL) is the most common malignancy in children[10], representing a highly aggressive disease in all age groups. Children with Down syndrome (DS) have a 10-20 fold increased risk of developing acute leukemia: both acute myeloid leukemia, particularly acute megakaryoblastic leukemia (AMKL) and B-cell precursor-ALL (BCP-ALL)[11]. Approximately 1 in 150 DS individuals develop leukemia implying that the gain of chromosome 21 alone is insufficient for leukemogenesis. However, there is evidence that it represents an early event in a multi-step process. For example, mutations of *GATA1* have been demonstrated to cooperate with trisomy 21 in transformation to DS-AMKL[12]. Recently, mutations within the *JAK2* pseudokinase domain have been described as a significant event in the development of BCP-ALL in DS[13-15].

Acquired genetic changes provide essential diagnostic and prognostic markers in ALL and are used in the risk stratification of patients for treatment[16]. Genomic studies

have discovered novel aberrations involving genes involved in B cell differentiation and cell cycle control which have been linked to prognosis and relapse in BCP-ALL[17-20]. Translocations involving the *immunoglobulin heavy chain locus*, *IGH@*, have been identified as a new cytogenetic subgroup in BCP-ALL at an incidence of approximately 3%, occurring predominantly among older children and young adults [21]. They result in juxtaposition of the *IGH@* transcriptional enhancers to genes on partner chromosomes, leading to their deregulated expression[21-24]. We have described deregulated expression of the type 1 cytokine receptor *erythropoietin receptor precursor*, *EPOR,* in two patients with BCP-ALL and the translocation, t(14;19)(q32;p13)[25]. Here we report the involvement of another cytokine receptor chain, *CRLF2,* through two novel genomic abnormalities which involve the pseudoautosomal region, PAR1, of both sex chromosomes in translocations and interstitial deletions, leading to deregulated *CRLF2* signaling.

Methods

Patients and cell lines

The BCP-ALL patients in this study were identified from the Leukaemia Research UK Cancer Cytogenetics Group Karyotype Database in Acute Leukaemia (n=89)[26] or other cytogenetic laboratories (n=9) and treated over a 17 year period (1991 to 2008). Informed consent was obtained in accordance with the Declaration of Helsinki.

Two BCP-ALL cell lines, MHH-CALL-4 and MUTZ5 (DSMZ, Germany) were grown in RPMI-1640 medium supplemented with 20% fetal calf serum and 1% glutamine (Sigma-Aldrich, UK) and maintained at 10^6 cells/ml.

Cytogenetics and Fluorescence *in situ* hybridisation

Cytogenetics and fluorescence *in situ* hybridization (FISH) were performed on the same diagnostic and relapse samples in patients and cell lines. The involvement of *IGH@* was determined by interphase FISH, using the LSI *IGH* Dual Color Break-Apart Rearrangement Probe (Abbott Diagnostics, Illinois, USA)[21]. Whole chromosome painting probes (wcpX and wcpY) (STAR*FISH Cambio, Cambridge, UK and MPBIO, Solon, USA) and specific probes were hybridized to identify the partner chromosome

and map the breakpoint positions on Xp and Yp[21]. Two alternative break-apart probes were designed to identify the involvement of *CRLF2* in the translocation, as indicated in Figure 1. The normal signal pattern for these and all other break-apart probes is 0 red, 0 green and 2 fusion signals (0R0G2F). A break-apart probe to *P2RY8* was designed to map the centromeric breakpoint of the deletion in patients with a deleted green signal from *CRLF2* Probe 1 (Figure 1). A commercial probe to *CDKN2A*: LSI® p16 (9p21) SpectrumOrange™/CEP® 9 SpectrumGreen™ (Abbott Diagnostics) or home grown probe was used to evaluate deletions on 9p[27]. Results were recorded using a fluorescence microscope (Ziess, Welwyn Garden City, UK) and digital imaging software from MetaSystems (Altlusheim, Germany) and Applied Imaging (Newcastle, UK).

Long-distance inverse PCR

Long distance inverse-PCR (LDI-PCR) from *IGHJ* for both patient and cell line samples was carried out as previously described[21]. Sequences were analyzed via University of California Santa Cruz Genome Bioinformatics database using BLAT (March 2006).

Quantitative real-time-PCR

Total cellular RNA was extracted from diagnostic patient samples with the translocation (n=7), with the deletion (n=5), controls without translocations or deletions (n=17), BCP-ALL cell lines with the translocation (n=2) and without (n=12). Quantitative real-time-PCR (qRTPCR) was performed using Applied Biosystems (California, USA) TaqMan® Gene Expression Assays (*CRLF2* assay ID Hs_00845692, *IL7RA* assay ID Hs_00902334, *IL2R*G assay ID Hs_00173950, GAPDH assay ID Hs_99999905 and *B2M* assay ID Hs_99999907), as previously described[21]. The comparative Ct method was used to quantify relative mRNA expression levels using the endogenous control genes *B2M* and *GAPDH*.

Cell surface expression of CRLF2

FACs

Staining for flow cytometry was performed in FACs buffer (PBS, 2mM EDTA and 1% BSA). Antibodies to CRLF2 (clone 1A6) and mouse IgG2a isotype control were obtained from eBiosciences (California, US). Acquisition of the data was performed on FACsDiva (BD Biosciences, Oxford, UK) and analysed with WinMDI (http://facs.scripps.edu/software.html).

Retroviral constructs

The human cDNA sequence for CRLF2 (hCRLF2) was cloned from a pMX-puro construct. The coding sequence, preceded by a Kozak consensus sequence was subcloned into a pcDNA3.1/myc-His vector (Invitrogen, Paisley, UK), then into a GFP bicistronic retroviral vector, MigRI, with BglII and HpaI restriction sites. Phoenix α packaging cell line was transfected with empty vector (EV) control and hCRLF2 containing plasmids by Calcium phosphate transfection. Viral supernatants were collected after 24h, 36h and 48h and stored at -80°C.

Colony forming cell (CFC) assay

Cells were harvested from fetal livers of E13.5 embryos from time-mated C57/BL6 mice. $4x10^6$ cells were transferred to a 6-well plate and centrifuged at 2300 rpm for 90 min in hCRLF2 or EV retroviral supernatants supplemented with stem cell factor (SCF, 50 ng/ml), FLT3 ligand (FLT3L, 10ng/ml) and IL7 (10ng/ml) (all cytokines from Peprotech, London, UK), three times over a period of 2 days. They were plated in a semi-solid, methylcellulose based medium (Stemcell Technologies, Grenoble, France) in triplicate to assess colony formation. The cytokines support differentiation only to pre-B cells ($CD43^+$, $B220^+$, $CD19^+$, IgM^-). On day 3, GFP positive cells were sorted on a FacsVantage with CellQuest software (Becton Dickinson, Oxford, UK) until $0.5x10^6$cells were collected. Cells were resuspended in 400μl Iscove's modified medium containing SCF, FLT3L and IL7 (Stemcell Technologies, Grenoble, France), 3.6 ml of the methylcellulose based medium was added and cells were evenly resuspended. After 5 min, 1.1ml suspension (containing $0.13x10^6$cells) was plated into 35mm dishes. Colonies were counted and cells replated every 8 days. Cells were collected by

centrifugation, counted and either snap-frozen for protein lysates, used for FACS staining or further plating.

Flow cytometry analysis for CFC assay

Cells ($1.5x10^5$) were stained for 1h on ice with saturating concentrations of anti-mouse CD43 PE labeled, anti-mouse CD19 PCy5 labeled or anti-mouse μ chain antibodies (eBiosciences, San Diego, USA). They were washed and resuspendend in PBS and analyzed on a FACSCanto with FacsDiva software (Becton Dickinson, Oxford, UK).

Transfection of BCP-ALL cell lines

Transfection was performed by Nucleofection (program X-05) using the Cell Line Nucleofector Kit V (Amaxa, Cologne, Germany) for the Nucleofector Device (Amaxa, Cologne, Germany), according to the manufacturer's protocol. Briefly, 1.5 $x10^6$ cells were transfected with 3µg of either pGIPZ control vector containing a scrambled, non-silencing shRNA sequence (cat: RHS4346) as a control or one of two different pGIPZ CRLF2 targeting shRNA plasmids (Open Biosystems, Alabama, USA).

MTS assay

Cell proliferation was determined using the CellTiter 96® AQueous Assay (Promega, Wisconsin, USA). Absorbance was recorded at 490 nm. Experiments were carried out in 96 well plates in triplicate with cells seeded at 10^5cells per well. Data were plotted to show the mean and standard error (n= 3), and subjected to statistical analysis using Graphpad Prism (Graphpad Software Inc.) and Student t-test.

JAK2 and STAT5 phosphorylation

Cells were harvested from the 2^{nd} plating and lyzed in buffer containing 1% Triton 100X, 10 mM Tris pH 7.5, 50 mM NaCl, 5mM EDTA, 20% glycerol in the presence of protease inhibitors (Boehringer Ingelheim GmbH, Germany) and 1mM sodium orthovanadate. Western blotting was performed using 100μg of cell lysates. Cell lines and CFC cell protein lysates were probed with anti-phospho JAK2 (Y1007/Y1008), anti-

phospho STAT5 (Tyr694) (Cell Signaling Technology, Inc., Danvers, MA, USA), anti-STAT5, anti-JAK2 (Santa Cruz Biotechnology Inc., CA, USA) and anti-β-actin and anti-CRLF2 (AF981) (R&D Systems, Abingdon, UK).

Knockdown of CRLF2

CRLF2 protein expression was knocked down in MUTZ5 using two short hairpin RNA (shRNA) (Open Biosystems): anti CRLF2 shRNA plasmids and control vector (cat: RHS4346); were transfected by nucleofection into MUTZ5. After 3-4 days in culture, 50ug of total protein lysates were prepared and probed with an antibody specific for CRLF2 (AF981, R&D systems). The growth of the cells was monitored using an MTS assay (Promega).

***CRLF2* mutational analysis**

PCR primers were designed to amplify *CRLF2* exons 1-6, using DSGene software (Accelrys, CA, USA). Genomic DNA from 9 patients and the 2 cells lines was amplified using Amplitaq Gold (Applied Biosystems, CA, USA) prior to denaturing high-performance liquid chromatography with Transgenomic patented separation DNASep® Cartridges for mutation detection (Transgenomic Wave system, NE, USA). Normal DNA samples (n=29) were used as negative controls. Amplicons with chromatographic profiles differing from wild-type were purified with the QIAquick PCR purification kit (Qiagen, Illinois, USA), sequenced by Geneservice (Cambridge, UK) and analysed using DSGene software.

***JAK2* mutational analysis**

Genomic DNA was extracted from samples fixed for cytogenetic analysis. Primers were used to amplify exon 14 of the *JAK2* gene as described previously[15]. PCR products were directly sequenced using BigDye Terminator sequencing chemistry (Applied Biosystems, California, USA) following direct purification of the PCR products by magnetic bead separation (Ampure, Agencourt, USA).

Genomic oligonucleotide arrays

DNA was extracted using either the Gentra or DNeasy blood and tissue kit (Qiagen, Illinois, USA). Array-based comparative genomic hybridization (aCGH) was performed on a Human Genome CGH Microarray 244A platform (7 patients and 2 cell lines), or a custom Human Genome CGH Microarray 105K platform (6 patients) with additional probes to the PAR1 region (Agilent Technologies, Santa Clara, USA). Test and sex-matched DNA (Promega, Wisconsin, USA) was hybridized to the arrays and scanned. Signal intensities from the generated images were measured using Feature Extraction 9.5.3 (Agilent Technologies) and imported into CGH Analytics v3.5.14 software packages (Agilent Technologies). Analysis of genomic gains and losses was performed using Spotfire DecisionSite Software for Functional Genomics (http://spotfire.tibco.com). All data is available upon request.

Results

Clinical and demographic data of patients with translocations and deletions involving *CRLF2*

We identified 97 BCP-ALL patients with chromosomal abnormalities involving PAR1, 33 with translocations, either t(X;14)(p22;q32) or t(Y;14)(p11;q32), and 64 with deletions, either del(X)(p22.33p22.33) or del(Y)(p11.32p11.32) (Table 1). An incidence of 0.8% for the translocations (accounting for approximately 23% of all *IGH@* translocations) and 4.2% for the deletions was determined by screening 1000 unselected cases of childhood ALL by FISH using the *CRLF2* specific probe 1 (Figure 1). The clinical and demographic features of these patients are summarized in Table 1 and detailed in Supplementary Table 1. For the cohort overall, the median age was 5.5yrs (range 1-76), their median white blood cell count (WBC) was $25x10^9$/L (range 1-400) and all were positive for CD10 and CD19. Apart from intrachromosomal amplification of chromosome 21 (iAMP21)[28,29], none of the patients in this study showed established chromosomal abnormalities of prognostic significance (high hyperdiploidy, rearrangements of *MLL* or *BCR-ABL1* and *ETV6-RUNX1* fusions) either from karyotyping or routine FISH screening[30]. iAMP21 patients accounted for 38% (11/29) of the non-DS patients with the deletion and 17% (11/64) of the iAMP21 cases tested.

The 33 patients with the translocations included 6 DS children and one patient with Klinefelter syndrome (L759/02). The median age at diagnosis for this group was older than expected for BCP-ALL, at 16 years (range 3-76) with a median WBC of $40x10^9$/L (range 1-342).

The 64 patients with interstitial deletions centromeric of *CRLF2* included 35 DS. The median age of this group of 4 years (range 1-35 years) was lower than those with the translocation, with a slightly lower median WBC of $22x10^9$/L (range 1-400). When divided into DS and non-DS the median age was 3 years (range 1-18) and 6 years (range 1-35 years), respectively. Among 68 DS patients tested, 35 (52%) had the deletion, while the remaining 33 patients (48%) (data not shown) without the deletion had a median age of 7.5 years (range 1-16 years) and WBC count of $8x10^9$/L (range 2-605).

Fluorescence *in situ* hybridization identifies translocations and deletions within PAR1

The cryptic translocations were identified by FISH using the probe to *IGH@*, with the positive result 1R1G1F (Figure 1a&c). A number of patients showed additional copies of the partner chromosomes, indicated from the signal pattern with this probe (Supplementary Table 1a). The involvement of the sex chromosomes in the translocations was identified by wcpX and wcpY (Figure 1b&d). Mapping by FISH using probes located along the short arms of the sex chromosomes confirmed that the translocation involved PAR1 and specifically the cytokine receptor, *CRLF2*, at Xp22 and Yp11. Break-apart probes (C*RLF2* probes 1 and 2) to *CRLF2* hybridized to the same samples (Figure 1e&g) showed the split signal patterns 1R1G1F (probe 1) (Figure 1e) and 1R1G1F or 0R1G2F (probe 2), which, in association with the positive result from the *IGH@* probe, confirmed the involvement of *CRLF2* in the reciprocal translocation. The signal patterns 1R1G2F and 1R2G1F (*CRLF2* probe 1) indicated that the translocation was associated with an additional normal or derived X chromosome, respectively. They were observed at a high incidence of 27% (n=9/33) among the translocation patients (Table 1). The loss of a green signal (1R0G1F) with *CRLF2* probe 1 indicated that, in association with the translocation, a cryptic deletion of the derived

sex chromosome was present within the region centromeric of *CRLF2*. This was detected in 25% (n=6/24) of patients tested with probe 1.

It is known that a high proportion of DS patients with ALL show gain of an X chromosome within the karyotypes of their leukemic blasts[31]. The observation that gain of X and/or DS (n=9, 27%; n=6, 18%, respectively) were predominant among this series of translocation patients, prompted us to test a further cohort of DS ALL in search of additional cases with these translocations. Among 68 other DS patients tested by FISH no additional patients with the translocation were identified; however 52% (n=35) showed deletion of the green signal centromeric of *CRLF2* in the absence of the translocation, of which 26% (n=9) also had the gain of an X chromosome. Prompted by these findings we tested non DS ALL patients with gain of X and gain/abnormality of chromosome 21: 29 patients were identified with this interstitial deletion. Its incidence was high at 38% (11/29 patients tested) in non DS patients with intrachromosomal amplification of chromosome 21 (iAMP21)[28,29] (Table 1 & Supplementary Table 1b).

FISH mapping the extent of the deletion indicates 5' *P2RY8* as the proximal breakpoint

Serial hybridization with probes located centromeric of *CRLF2* identified that the deletion incorporated the *IL3RA* and *CSF2RA* genes and defined the proximal breakpoint as the 5' centromeric end of the *G-protein coupled purinergic receptor P2Y8*, *P2RY8*. The signal pattern 0R1G1F with the *P2RY8* break-apart probe denoted a telomeric deletion of the 3' portion of this gene (Figure 1f&h) and confirmed this breakpoint in 62 of the patients with this deletion (translocation patients (n=5), deletion patients (n=57) with one translocation patient (10692) harboring a different proximal breakpoint**.** (Supplementary Tables 1a&b). The signal patterns from this probe, in combination with *CRLF2* probe 1, defined both the proximal and distal breakpoint of this interstitial deletion, respectively. Metaphases analysis showed that the red signal of the *CRLF2* probe and/or the green signal of the *P2RY8* probe were retained on the sex chromosome, ruling out the presence of an unbalanced translocation.

Long distance inverse PCR confirmed the involvement of *CRLF2*

LDI-PCR confirmed the involvement of *CRLF2* in 11 translocation patient samples and two cell lines, MHH-CALL-4 and MUTZ5, with unbalanced t(Y;14) translocations. The breakpoints were clustered within a 27kb region (summarized in Figure 1i, breakpoint details are provided within Supplementary Table1a and summarized in Supplementary Table 2). The translocation juxtaposes the *IGHJ* segments to the region immediately centromeric of *CRLF2*, whilst, as all other *IGH@* translocations, not affecting the coding region of the gene. The primary sequence data from the 11 patients and 2 cell lines is provided in Supplementary Figure 1. Sequencing traces are available in the DDBJ/EMBL/GenBank nucleotide sequence databases: accession numbers: AB506477, AB506478, AB506479, AB506480, AB506481, AB506482, AB506483, AB506484, AB506485, AB506486 and AB506487.

Quantitative real-time-PCR and flow cytometry showed over-expression of CRLF2 mRNA and protein.

qRTPCR showed an increase in *CRLF2* mRNA expression in samples from patients and cell lines with the translocation (n=7 and n=2, respectively) and deletion (n=5) (Figures 2ai-iii). mRNA levels were increased from 80 to >1,500 fold in the translocation patients and from 3500 to >7000 fold in the cell lines, compared to the mean of the patient controls or cell line controls, respectively (Figure 2ai&ii). Samples from patients with the deletion also showed a significant increase in CRLF2 expression from 5 to100 fold, although at a lower level than the translocation patients when compared to the same controls (Figure 2aiii). Due to the heterodimeric nature of the IL7 and TSLP receptors, we assessed the mRNA levels of *IL7RA* and *IL2RG* in patients and cell lines with the translocation. Both were apparently normally expressed (Figures 2b&c). A high CRLF2 protein expression was confirmed by flow cytometry, which measured relative cell surface CRLF2 expression in the 2 cell lines compared to 4 control ALL cell lines (Figure 2e).

Western blotting for pSTAT5 and pJAK2 suggests activation of the JAK-STAT pathway

Intracellular signaling from the wildtype TSLP receptor is thought to lead to STAT5 activation, possibly following JAK2 activation. The phosphorylation status of JAK2 and STAT5 was investigated by western blot analysis of extracts from the two BCP-ALL cell lines, MHH-CALL-4 and MUTZ5. Both showed phosphorylated JAK2 and STAT5 indicating the activation of this pathway (Figure 2f).

Retrovirus-mediated expression of CRLF2 stimulates the growth of primary lymphoid progenitors

The effect of CRLF2 on proliferation of primary lymphoid progenitors was assessed by colony formation of mouse fetal liver cells infected with hCRLF2. The cytokines added to the medium support differentiation only to pre-B cells ($CD43^+$, $B220^+$, $CD19^+$, IgM^-) and ~95% of cells in culture were $CD43^+/B220^+$ from 1st plating, with little contamination from $CD13^+$ myeloid cells (~1-2%, not shown). After 8 days in culture, colonies from hCLRF2 expressing cells were significantly higher in number (unpaired Student t-test, 1st and 2nd plating $p<0.0001$, 3rd plating $p< 0.0009$) and larger in diameter compared to EV controls (Figures 3a&b). These differences were consistent for all passages. Differences were most pronounced for the 3rd plating. hCRLF2 expressing cells continued to proliferate in the 4th plating, while EV did not.

To assess whether CRLF2 was mediating the increased proliferation through STAT5 activation, cells from the 2nd plating were lysed and STAT5 phosphorylation evaluated by western blotting (Figure 3c). STAT5 phosphorylation at Tyr 694 was increased in hCRLF2 positive cells compared to EV cells, while no differences were observed in total STAT5 levels.

A higher proportion of hCRLF2 expressing cells showed a less differentiated phenotype compared to EV cells. This was indicated by the presence of a higher number of $CD43^+/CD19^+$ pre-B cells in EV colonies (87.3%) than in hCRLF2 colonies (60%), implicating that the increased proliferation was accompanied by maintenance of a larger pool of cells with an immature $CD43^+/B220^+/CD19^-$ phenotype (Figure 3d). This was confirmed within the hCRLF2 positive population; colonies with lower expression had a higher proportion of $CD43^+/CD19^+$ cells (81%) compared to those with high expression of CRLF2, whose $CD43^+/CD19^+$ population was only 23% of the total

(Figure 3e). These data suggest that activation of STAT5 accompanies the over-expression of CRLF2 in B-lymphoid progenitor transformation and that its effect is most pronounced in early B-cell precursors.

Knockdown of CRLF2 decreases proliferation

To demonstrate that CRLF2 expression plays a role in cellular transformation, CRLF2 protein expression was knocked down in the MUTZ5 cell line using shRNA. There was an appreciable decrease in protein expression in cells transfected with anti CRLF2 shRNA plasmid compared with cells transfected with a scrambled control vector (Figure 3f). Knockdown of CRLF2 resulted in a decrease in the growth of these cells measured using an MTS assay ($p=0.0288$, unpaired Student t-test) (Figure 3g). However the proliferation was not reduced to the extent that would be expected to correlate with the substantially decreased protein level. Taken together, these results show that although CRLF2 over-expression triggers cell survival and growth, it is insufficient to fully transform primary cells. To further investigate this hypothesis, we searched for cooperating mutations.

DS patients with translocations or deletions showed JAK2 mutations

Among 17 DS patients tested for mutations within the *JAK2* pseudokinase domain, 60% (n=11, 2 with the translocation and 9 with the deletion) showed the specific acquired mutation, *JAK2*R683 [R683G (n=8), R683S (n=2), insertion mutation (n=1)] (Table 1 & Supplementary Tables 1a&b). In one patient (20033) with the translocation seen at diagnosis and relapse, the *JAK2* mutation was found only in the relapse sample. As these mutations were identified in DS ALL patients with the translocation or deletion, they indicate a potential oncogenic collaboration between CRLF2 over-expression and JAK2 mutation. The two cell lines also showed misense mutations of *JAK2*. MUTZ5 showed the *JAK2*R683G, while MHH-CALL-4 showed an alternative mutation within the pseudokinase domain: *JAK2*I682F.

CRLF2 mutation screening reveals SNP but no somatic mutations

A preliminary mutational screen of *CRLF2* exons, encoding proposed extracellular and transmembrane domains, in patients (n=9) (4 with the translocation, 5 with deletion) and normal individuals (n=29), revealed A11A (translocation n=3, deletion n=4 and controls n=5), V136M (translocation n=1 and controls n=3) and P122P (translocation n=1). These represent single nucleotide polymorphisms rather then somatic mutations. A non-synonymous amino acid change, V244M, was seen in both the MHH-CALL-4 and MUTZ5 cell lines.

Genomic analysis of translocation and deletion patients reveals deletions of genes common to other BCP-ALL

To investigate the global genomic copy number alterations associated with the translocations and deletions, aCGH was carried out on available translocation (n=7) and deletion (n=6) patient samples, as well as the cell lines with the translocation (n=2) (Figure 4) (detailed in Supplementary Table 3). For translocation patient 11687, matched diagnostic and relapse samples were available.

Copy number changes were observed in all samples. Four DS patients (4318, 6119, 9534 and 11538) clearly showed gain of chromosome 21 corresponding to their constitutional karyotypes. Patient 6119 had an additional acquired chromosome 21. None of the other patients or the two cell lines showed copy number changes involving chromosome 21. Recurrent focal and whole gene deletions of C*DKN2A*, *PAX5* and *IKZF1* were identified in both the translocation and deletion patients (Figure 4 and Table 1, with details of genomic breakpoints and summary of the extent of the deletions in Supplementary Tables 3&4, respectively). *CDKN2A* was deleted in 100% (7/7) of translocation and 83% (5/6) of deletion patients. *CDKN2A* deletions detected by aCGH were confirmed by FISH in 5 cases, while focal deletions were seen in a further 4 patients by aCGH only, which were too small to be detected by FISH. In total *CDKN2A* deletions were identified in 54% (14/26, 10 monoallelic and 4 biallelic deletions) of cases tested by FISH. In addition, the cell lines, MHH-CALL-4 and MUTZ5, were normal and showed a biallelic deletion, respectively, by FISH. In the translocation patients, *PAX5* was deleted in 43% (3/7) and *IKZF1* in 71% (5/7). Conversely, *PAX5* deletions were more frequent in the deletion patients than *IKZF1* deletions; 66% (4/6) and 50%

(3/6), respectively. Deletions involving all 3 loci were observed in the 2 cell lines. Deletions of the known cancer genes, *RB1* (2 translocation patients, 2 deletion patients and MUTZ5) and *FHIT* (1 patient with the X chromosome deletion, diagnostic and relapse samples of translocation patient, 11687) were also detected, albeit at low frequency. Overall a higher number of copy number alterations were seen in the diagnostic compared to the relapse sample from patient 11687, but C*DKN2A*, *PAX5* and *IKZF1* deletions were common to both samples. These results indicate that the subset of patients with deregulated CRLF2 show a pattern of oncogenic events similar to other BCP-ALL. Attempts to customize the standard 105K arrays with oligonucleotides targeting PAR1 were unsuccessful due to high background noise from these probes. Therefore, it was not possible to delineate the boundaries of the deletion.

Discussion

The involvement of cytokine receptors and *JAK* kinases is being increasingly reported to play a role in the pathogenesis of BCP-ALL[14,15,25]. In this study, we have provided substantial support for this function and evidence of the involvement of the CRLF2 signaling pathway in a lymphoid malignancy from the identification of its deregulated expression. Its over-expression arises from a translocation juxtaposing *CRLF2* to the *IGH@* enhancer or an interstitial deletion. In cases with both the translocation and the deletion, the deletion is unlikely to have an additive effect on CRLF2 expression because, as a result of the translocation, the entire *CRLF2* gene has relocated to the derived chromosome 14, while the deletion is located to the derived sex chromosome. Although we were unable to accurately delineate the deletion boundaries by aCGH, data from single nucleotide polymorphism (SNP) arrays of a similar deletion involving *CSF2RA* and *IL3RA*, indicated that the breakpoints were variable between patients[18]. Nevertheless, one possible explanation for the deregulated expression of CRLF2 in these cases could be that, as a result of the deletion, *CRLF2* may become juxtaposed within the region of the gene promoter of *P2RY8, SFRS17A or ASMT*. The *P2RY8* promoter has previously been described to be involved in promoter swapping with one of the Sry (sex-determining region Y)-box genes (*SOX5*) on chromosome 12 in a patient with primary splenic follicular lymphoma[32]. Deletions of the PAR1 region,

including *CSF2RA* and *CRLF2,* have been reported in mantle cell lymphoma[32]. However, to our knowledge, there are no reports of an acquired, activating chromosomal abnormality within PAR1 in BCP-ALL to date.

In this study, over-expression of CRLF2 was found to occur at a high incidence in DS-ALL patients. Among the DS-ALL patients over-expressing CRLF2 tested, the majority had mutations targeting the *JAK2* pseudokinase domain, *JAK2*R683[13-15]. These observations suggest an oncogenic cooperation between the two events. Interestingly, this particular cooperation resembles the situation in human myeloproliferative syndromes involving the thrombopoietin receptor, *MPL*, one of several *JAK2* receptors, and *JAK2* mutations[33]. The two cell lines, MHH-CALL-4 and MUTZ5, derived from non DS BCP-ALL, showed mutations within the *JAK2* pseudokinase domain. These findings indicated that the occurrence of *JAK2* mutations is not restricted to DS-ALL patients, as recently confirmed by others[34]. Although CRLF2 protein expression was substantially knocked down in the cell lines, proliferation was decreased by only a small amount. The subsequent finding of *JAK2* mutations in the cell lines may explain, in part, the reduced ability to decrease proliferation, as the JAK-STAT signaling may be protected from inactivation by, at least, this additional mechanism. There was no evidence of activating somatic mutations of *CRLF2* in DS and non DS patients with the translocation or deletion.

Our results add important information to the role of the IL7-TSLP receptor signaling pathway in lymphoid development. These two cytokine receptors are dimeric, share IL7R and use IL2RG and CRLF2, respectively, to form heterodimers. Inactivation of *JAK3*, *IL2RG* and *IL7R* has been described in patients with severe combined immunodeficiency[2]. Here we demonstrate that CRLF2 signaling, normally involved in the control of the cellular response to inflammatory and allergic stimuli, is also involved in malignant lymphoid transformation. To what extent the intracellular signaling is similar in both situations is to be further investigated.

The majority of these BCP-ALL patients showed a relatively simple karyotype, in which the translocation represented a primary cytogenetic change with the frequent gain of a normal or derived X chromosome. The deletion showed evidence of association with iAMP21. However, aCGH analysis showed that both translocation and deletion

patients shared cryptic deletions of the B-cell differentiation and cell cycle control genes in common with other BCP-ALL[17]. The high incidence of *CDKN2A* deletions implicates cooperation between deregulated CRLF2 and $p16^{INK}$ expression.

Interestingly, those patients with the translocation had a higher median age than those with the deletion. This is in agreement with the older age described for patients with other *IGH@* translocations[21]. A detailed survival analysis based on a large cohort treated on a single protocol is needed to determine the clinical relevance of these abnormalities.

In conclusion, we have shown that over-expression of CRLF2 is associated with activation of STAT5 in cell lines and transduced primary B-cell progenitors. CRLF2 expression also had the effect of increasing growth of immature B-cell precursors, when mouse fetal liver cells were used as a model for lymphoid progenitors. These factors indicate a causal role of CRLF2 over-expression in lymphoid transformation. These important observations pave the way for a systematic study of ALL for mutations of those genes encoding signaling molecules involved in this pathway. Thus patients with deregulated CRLF2 expression are emerging as a distinct subgroup of BCP-ALL, providing potential molecular targets for therapy.

Acknowledgements

The authors thank all the clinicians for providing samples and clinical data, the members of the UK Cancer Cytogenetics Group for cytogenetic data, Clinical Trial Service Unit, University of Oxford, UK, for clinical data and UK Children's Cancer and Leukaemia Group, Leukaemia and Lymphoma Division and Adult Leukemia Working Party members, who designed and coordinated the clinical trials through which these patients were identified and treated. The authors are grateful to Dr. T. Kitamura, University of Tokyo, Tokyo, Japan, for providing the pMX-puro construct.

This work was supported by Leukaemia Research (London, UK), Medical Research Council (London, UK), Hope Foundation for Cancer Research (UK), Deutsche Krebshilfe (Bonn, Germany), and Kinder-Krebs-Initiative Buchholz/Holm-Seppensen (Buchholz, Germany).

Authorship contributions

LJR, MC and IV contributed equally to this work. The laboratories of MJSD, RS and CJH contributed equally to this work. LJR, MC, MJSD, RS and CJH designed the research and wrote the paper. AVM, OAB, JCS and OH designed some aspects of the research. LJR, MC, IV, TA, MJC, TC, EC, SG, MG, DSG, CH, LH, JI, LK, FNK, LM, LM, AM, HM, VR, CS and HT carried out the experiments and analyzed the data. All authors critically reviewed the manuscript.

Conflict of interest disclosure

The authors declare no competing financial interests.

References

1. Heim MH. The Jak-STAT pathway: cytokine signalling from the receptor to the nucleus. *J Recept Signal Transduct Res.* 1999;19:75-120.
2. Kovanen PE, Leonard WJ. Cytokines and immunodeficiency diseases: critical roles of the gamma(c)-dependent cytokines interleukins 2, 4, 7, 9, 15, and 21, and their signaling pathways. *Immunol Rev.* 2004;202:67-83.
3. Palmer MJ, Mahajan VS, Trajman LC, Irvine DJ, Lauffenburger DA, Chen J. Interleukin-7 receptor signaling network: an integrated systems perspective. *Cell Mol Immunol.* 2008;5:79-89.
4. Rochman Y, Leonard WJ. Thymic stromal lymphopoietin: a new cytokine in asthma. *Curr Opin Pharmacol.* 2008;8:249-254.
5. Ziegler SF, Liu YJ. Thymic stromal lymphopoietin in normal and pathogenic T cell development and function. *Nat Immunol.* 2006;7:709-714.
6. Hofmeister R, Khaled AR, Benbernou N, Rajnavolgyi E, Muegge K, Durum SK. Interleukin-7: physiological roles and mechanisms of action. *Cytokine Growth Factor Rev.* 1999;10:41-60.
7. Fujio K, Nosaka T, Kojima T, et al. Molecular cloning of a novel type 1 cytokine receptor similar to the common gamma chain. *Blood.* 2000;95:2204-2210.
8. Hiroyama T, Iwama A, Morita Y, Nakamura Y, Shibuya A, Nakauchi H. Molecular cloning and characterization of CRLM-2, a novel type I cytokine receptor preferentially expressed in hematopoietic cells. *Biochem Biophys Res Commun.* 2000;272:224-229.
9. Carpino N, Thierfelder WE, Chang MS, et al. Absence of an essential role for thymic stromal lymphopoietin receptor in murine B-cell development. *Mol Cell Biol.* 2004;24:2584-2592.
10. UK Childhood Cancer Study Investigators. The United Kingdom Childhood Cancer Study: objectives, materials and methods. *Br J Cancer.* 2000;82:1073-1102.
11. Zipursky A, Poon A, Doyle J. Leukemia in Down syndrome: a review. *Pediatr Hematol Oncol.* 1992;9:139-149.

12. Mundschau G, Gurbuxani S, Gamis AS, Greene ME, Arceci RJ, Crispino JD. Mutagenesis of GATA1 is an initiating event in Down syndrome leukemogenesis. *Blood*. 2003;101:4298-4300.
13. Malinge S, Ben-Abdelali R, Settegrana C, et al. Novel activating JAK2 mutation in a patient with Down syndrome and B-cell precursor acute lymphoblastic leukemia. *Blood.* 2007;109:2202-2204.
14. Bercovich D, Ganmore I, Scott LM, et al. Mutations of JAK2 in acute lymphoblastic leukaemias associated with Down's syndrome. *Lancet.* 2008;372:1484-1492.
15. Kearney L, Gonzalez De Castro D, Yeung J, et al. Specific JAK2 mutation (JAK2R683) and multiple gene deletions in Down syndrome acute lymphoblastic leukemia. *Blood.* 2009;113:646-648.
16. Harrison CJ. Cytogenetics of paediatric and adolescent acute lymphoblastic leukaemia. *Br J Haematol.* 2009;144:147-156.
17. Mullighan CG, Goorha S, Radtke I, et al. Genome-wide analysis of genetic alterations in acute lymphoblastic leukaemia. *Nature.* 2007;446:758-764.
18. Mullighan CG, Phillips LA, Su X, et al. Genomic analysis of the clonal origins of relapsed acute lymphoblastic leukemia. *Science.* 2008;322:1377-1380.
19. Mullighan CG, Su X, Zhang J, et al. Deletion of IKZF1 and prognosis in acute lymphoblastic leukemia. *N Engl J Med.* 2009;360:470-480.
20. Kuiper RP, Schoenmakers EF, van Reijmersdal SV, et al. High-resolution genomic profiling of childhood ALL reveals novel recurrent genetic lesions affecting pathways involved in lymphocyte differentiation and cell cycle progression. *Leukemia.* 2007;21:1258-1266.
21. Akasaka T, Balasas T, Russell LJ, et al. Five members of the CEBP transcription factor family are targeted by recurrent IGH translocations in B-cell precursor acute lymphoblastic leukemia (BCP-ALL). *Blood.* 2007;109:3451-3461.
22. Chapiro E, Russell L, Radford-Weiss I, et al. Overexpression of CEBPA resulting from the translocation t(14;19)(q32;q13) of human precursor B acute lymphoblastic leukemia. *Blood.* 2006;10 3560-3563.
23. Bellido M, Aventin A, Lasa A, et al. Id4 is deregulated by a t(6;14)(p22;q32) chromosomal translocation in a B-cell lineage acute lymphoblastic leukemia. *Haematologica.* 2003;88:994-1001.
24. Russell LJ, Akasaka T, Majid A, et al. t(6;14)(p22;q32): a new recurrent IGH@ translocation involving ID4 in B-cell precursor acute lymphoblastic leukemia (BCP-ALL). *Blood.* 2008;111:387-391.
25. Russell LJ, De Castro DG, Griffiths M, et al. A novel translocation, t(14;19)(q32;p13), involving IGH@ and the cytokine receptor for erythropoietin. *Leukemia.* 2009;23:614-617.
26. Harrison CJ, Martineau M, Secker-Walker LM. The Leukaemia Research Fund/United Kingdom Cancer Cytogenetics Group Karyotype Database in acute lymphoblastic leukaemia: a valuable resource for patient management. *Br J Haematol.* 2001;113:3-10.
27. Sulong S, Moorman AV, Irving JA, et al. A comprehensive analysis of the CDKN2A gene in childhood acute lymphoblastic leukemia reveals genomic deletion,

copy number neutral loss of heterozygosity, and association with specific cytogenetic subgroups. *Blood.* 2009;113:100-107.
28. Harewood L, Robinson H, Harris R, et al. Amplification of AML1 on a duplicated chromosome 21 in acute lymphoblastic leukemia: a study of 20 cases. *Leukemia.* 2003;17:547-553.
29. Moorman AV, Richards SM, Robinson HM, et al. Prognosis of children with acute lymphoblastic leukemia (ALL) and intrachromosomal amplification of chromosome 21 (iAMP21). *Blood.* 2007;109:2327-2330.
30. Harrison CJ, Moorman AV, Barber KE, et al. Interphase molecular cytogenetic screening for chromosomal abnormalities of prognostic significance in childhood acute lymphoblastic leukaemia: a UK Cancer Cytogenetics Group Study. *Br J Haematol.* 2005;129:520-530.
31. Forestier E, Izraeli S, Beverloo B, et al. Cytogenetic features of acute lymphoblastic and myeloid leukemias in pediatric patients with Down syndrome: an iBFM-SG study. *Blood.* 2008;111:1575-1583.
32. Nielander I, Martin-Subero JI, Wagner F, et al. Recurrent loss of the Y chromosome and homozygous deletions within the pseudoautosomal region 1: association with male predominance in mantle cell lymphoma. *Haematologica.* 2008;93:949-950.
33. Lasho TL, Pardanani A, McClure RF, et al. Concurrent MPL515 and JAK2V617F mutations in myelofibrosis: chronology of clonal emergence and changes in mutant allele burden over time. *Br J Haematol.* 2006;135:683-687.
34. Mullighan CG, Zhang J, Harvey RC, et al. JAK mutations in high-risk childhood acute lymphoblastic leukemia. *Proc Natl Acad Sci U S A*. 2009;106:9414-9418.

Table 1: Summary of patient demographic and genetic results.

		Total	Translocation	Deletion
Total	**Number**	97	33	64
	Median Age (range)	5.5 (1-76)	16 (3-76)	4 (1-35)
	Median WBC ($x10^9$/L) (range)	24.5 (1-400)	40 (1-342)	22 (1-400)
	Additional X	36/97 (37%)	9/33 (27%)	27/64* (42%)
	iAMP21	11/97 (11%)	0/33 (0%)	11/64 (17%)
	JAK2 mutation	11/24 (46%)	2/7 (29%)	9/17 (53%)
	CDKN2A deletions	22/36# (61%)	17/30# (57%)	5/6^ (83%)
	PAX5 deletions	7/13^ (54%)	3/7^ (43%)	4/6^ (66%)
	IKZF1 deletions	8/13^ (62%)	5/7^ (71%)	3/6^ (50%)
DS-ALL	**Number**	41/97	6/33	35/64
	Median Age (range)	3.5 (1-16)	16 (4-16)	3 (1-16)
	Median WBC ($x10^9$/L) (range)	23.5 (2-400)	22 (6-105)	25 (2-400)
	Additional X	17/41 (42%)	2/6 (33%)	15/35* (43%)
	iAMP21	0/41 (0%)	0/6 (0%)	0/35 (0%)
	JAK2 mutation	11/24 (46%)	2/7 (29%)	9/17 (53%)
	CDKN2A deletions	7/36# (19%)	2/30¤ (6%)	5/6^ (83%)

	PAX5 deletions	4/13^ (31%)	0/7^ (0%)	4/6^ (66%)
	IKZF1 deletions	3/13^ (23%)	0/7^ (0%)	3/6^ (50%)
Non-DS-ALL	**Number**	56/97	27/33	29/64
	Median Age (range)	8 (1-76)	17 (3-76)	8 (1-15)
	Median WBC ($x10^9$/L) (range)	24(1-342)	40 (1-342)	6 (2-205)
	Additional X	19/56 (34%)	7/27 (26%)	12/29* (41%)
	iAMP21	11/56 (20%)	0/27 (0%)	11/29 (38%)
	JAK2 mutation	ND	ND	ND
	CDKN2A deletions	15/36# (42%)	15/30# (50%)	0/6^ (0%)
	PAX5 deletions	3/13^ (23%)	3/7^ (43%)	0/6^ (0%)
	IKZF1 deletions	5/13^ (39%)	5/7^ (71%)	0/6^ (0%)

* Includes patients with +X identified by conventional cytogenetics and/or FISH
# CDKN2A deletions detected by aCGH and FISH
^ Abnormality identified by aCGH only
¤ CDKN2A deletion detected by FISH only

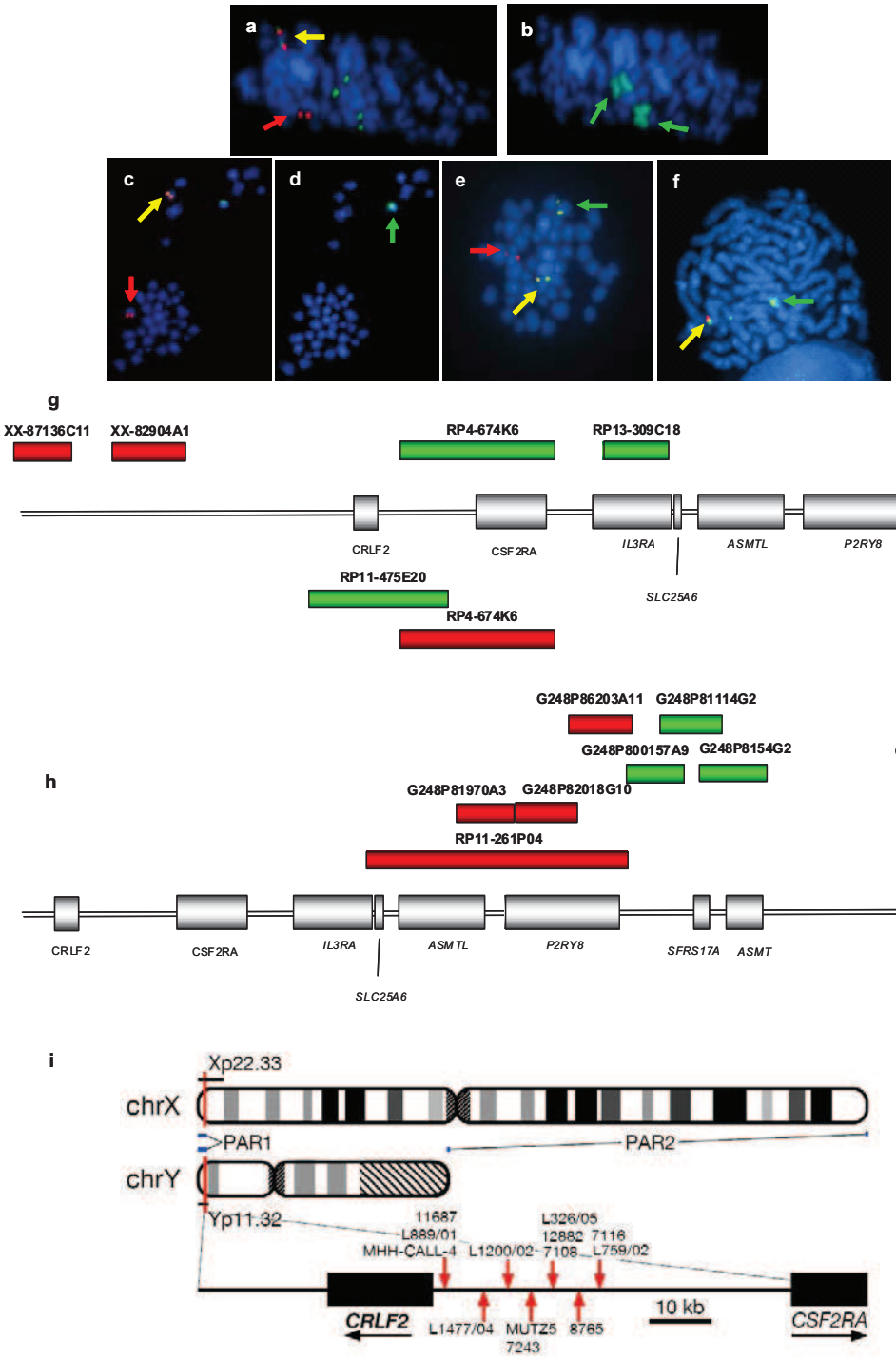
a
b
c
d
e
f
g
XX-87136C11
XX-82904A1
RP4-674K6
RP13-309C18
CRLF2
CSF2RA
IL3RA
ASMTL
P2RY8
SFRS17A
SLC25A6
RP11-475E20
RP4-674K6
h
G248P86203A11
G248P81114G2
G248P800157A9
G248P8154G2
G248P87990D1
G248P81970A3
G248P82018G10
RP11-261P04
CRLF2
CSF2RA
IL3RA
ASMTL
P2RY8
SFRS17A
ASMT
SLC25A6
~20kb
i
Xp22.33
chrX
PAR1
PAR2
chrY
Yp11.32
11687
L889/01
MHH-CALL-4
L1200/02
L326/05
12882
7108
7116
L759/02
CRLF2
L1477/04
MUTZ5
7243
8765
10 kb
CSF2RA

Figure 1. Involvement of *IGH@* and *CRLF2*

The same metaphases from a patient with t(X;14) (**a&b**) and one with t(Y;14) (**c&d**) showing a positive result with the *IGH@* probe: normal chromosome 14 (yellow arrows), derived chromosome 14 [der(14)] (red arrows) (**a&c**); involvement of the X chromosomes (wcpX) (green arrows on der(X)x2) (**b**), involvement of Y chromosome (wcpY) (green arrow) (**d**).

Representative metaphase hybridized with *CRLF2* probe 1 showing the translocation (**e**) normal X (yellow arrow), der(14) (red arrow), der(X) (green arrow).Representative metaphase hybridized with the probe to *P2RY8* showing the deletion (**f**): normal X (yellow arrow), X with deletion of red signal covering 3' *P2RY8* (green arrow). Magnification x~1000

FISH probe designs for break-apart probes to *CRLF2*, probes 1 and 2 (**g**) and *P2RY8* (**h**). (**g**) The red and green boxes above the schematic representation of PAR1 show the clones (Welcome Trust Sanger Institute) used in the design of *CRLF2* probe 1 (clone names given above each bar). The red and green boxes below the schematic indicate the clones (Invitrogen, Karlsruhe, Germany) used in the design of *CRLF2* probe 2. (**h**) FISH probe design for *P2RY8* . Fosmid and BAC clone names are given above each bar.

(**i**) Idiograms of X and Y chromosome showing the location of the PAR1 region. Breakpoint locations cloned by LDI-PCR from *IGHJ* segments are marked with red arrows.

a. CRLF2 mRNA expression

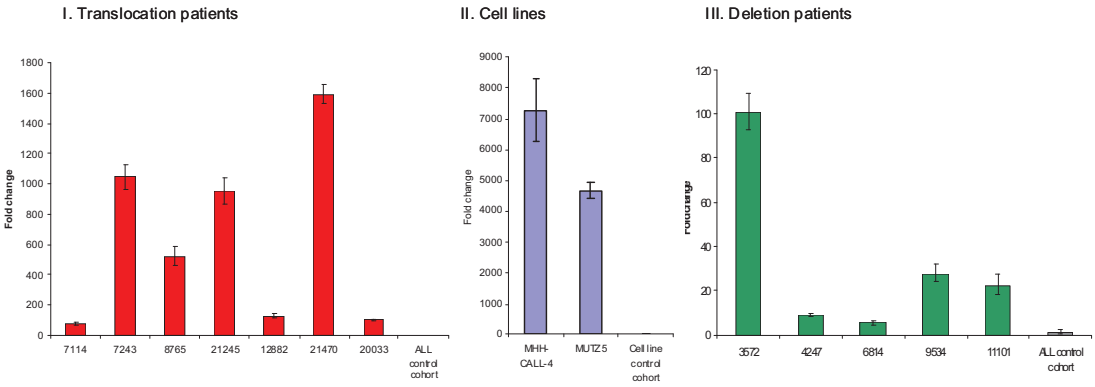

b. IL7RA and IL2RG mRNA expression in translocation patients

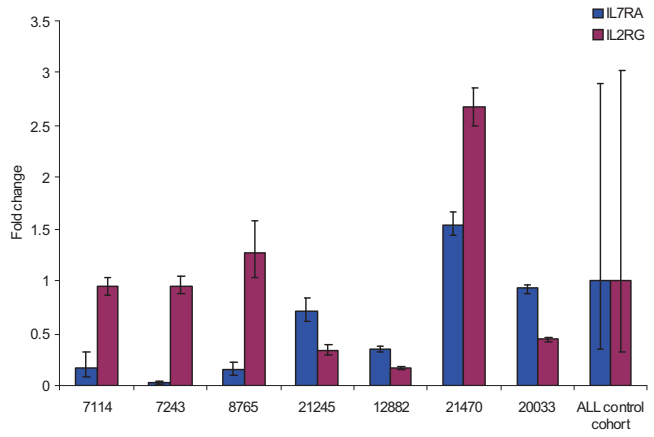

c. IL7RA and IL2RG mRNA expression in BCP-ALL cell lines

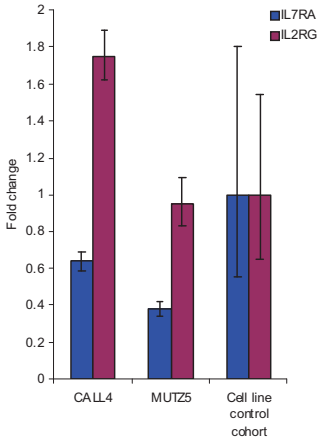

e

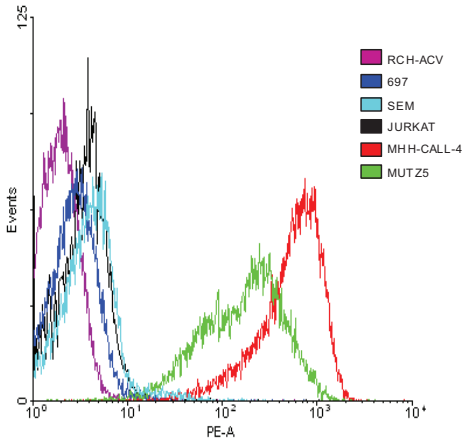

g

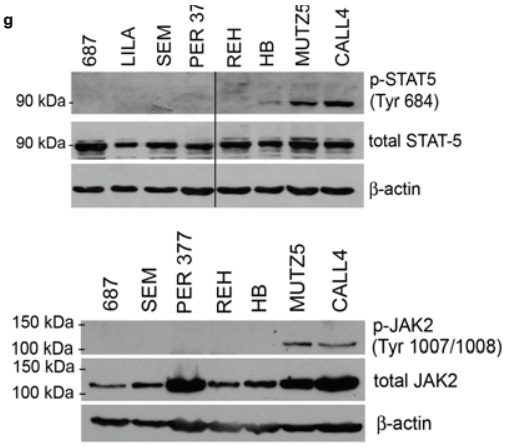

Figure 2. CRLF2, IL7RA and IL2RG expression and activation of the JAK-STAT pathway.

(**a**) Fold change of mRNA expression measured by the comparative Ct method of *CRLF2* in (i) translocation patient samples (n=7) compared to control patient cohort (n=17) without the translocation or deletion (ii) Cell lines (n=2) with the translocation compared to cell line control cohort (n=12): RCH-ACV, REH, Per365, 697, 380, Tanoue, LILA-1, SEM, LK63 (BCP-ALL) RAJI, DHL4 (B-cell lymphoma) and HL-60 (acute myeloid leukaemia) without the translocation or deletion and (iii) deletion patient samples (n=5) compared to the same patient control cohort (n=17).

IL7RA and *IL2RG* mRNA expression measured in (**b**) 7 patients with the translocation compared to the patient control cohort (**c**) the cell lines (n=2) compared to a cell line control cohort. The error bars for the control cohorts indicate the variable expression of all target genes tested.

(**f**) Flow cytometry histogram of control cell lines; RCH-ACV; 697; SEM; JURKAT and translocation positive cell lines: MHH- CALL-4 and MUTZ5 using a PE labeled antibody to CRLF2.

(**g**) Western blot showing presence of phosphorylated STAT5 and JAK2 observed in translocation positive cell lines, MHH-CALL-4 and MUTZ5, compared to other cell lines.

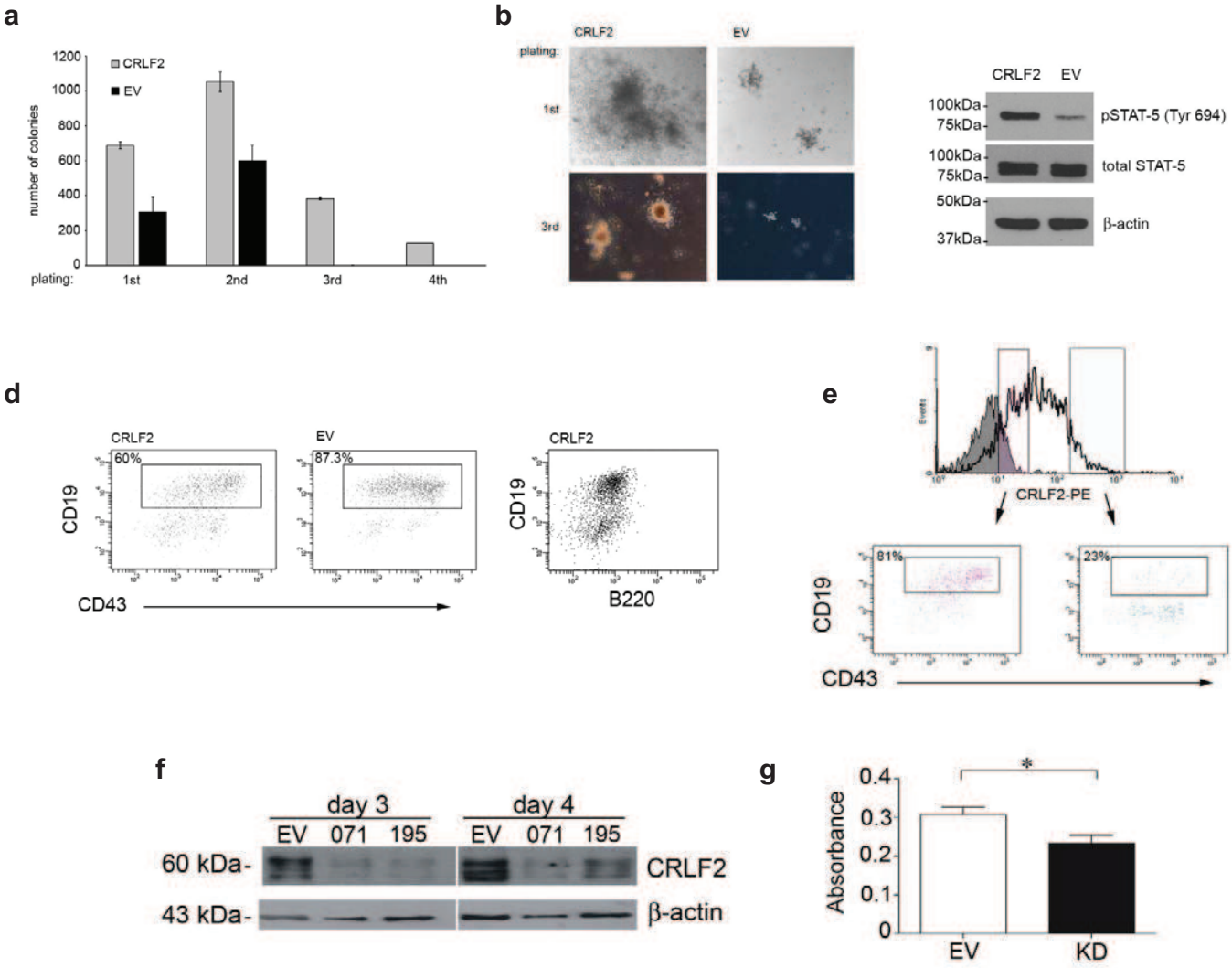
a
number of colonies
1200
1000
800
600
400
200
0
CRLF2
EV
plating:
1st
2nd
3rd
4th
b
CRLF2
EV
plating:
1st
3rd
CRLF2
EV
100kDa
75kDa
pSTAT-5 (Tyr 694)
100kDa
75kDa
total STAT-5
50kDa
37kDa
β-actin
d
CRLF2
60%
EV
87.3%
CD19
CD43
CRLF2
CD19
B220
e
CRLF2-PE
81%
23%
CD19
CD43
f
day 3
day 4
EV
071
195
EV
071
195
60 kDa-
CRLF2
43 kDa-
β-actin
g
Absorbance
0.4
0.3
0.2
0.1
0
*
EV
KD

Figure 3. Retroviral overexpression of *CRLF2* in haematopoietic progenitors results in increased proliferation and STAT-5 phosphorylation. Conversely, knockdown of CRLF2 results in decreased proliferation.

(**a**) CFC assay on E13.5 mouse fetal liver cells infected with hCRLF2 or EV control retroviruses and grown in methylcellulose semi-solid medium supplemented with IL-7, SCF and FLT3L. Values are average of two independent experiments; error bars indicate standard deviations (SD). All four platings show statistical significance between EV and hCRLF2 for number of colonies (unpaired student's t-test, 1^{st} and 2^{nd} plating $p<0.0001$, 3^{rd} plating $p< 0.0009$), only hCFL2 colonies grew in 4^{th} replating. EV colonies represented 44.9% ± 13.3%, 57.1% ± 11.2% and 0.43% ± 0.3% of the number of CRLF2 colonies at 1^{st}, 2^{nd} and 3^{rd} plating, respectively. (**b**) images showing relative sizes of colonies formed by hCRLF2 and EV transduced hematopoietic progenitors at two platings. (**c**) Lysed hCRLF2 infected cells from 2^{nd} plating have increased STAT-5 Y694 phosphorylation compared to EV cells. (**d**) A higher proportion of *CRLF2* over-expressing cells at 2^{nd} plating show less differentiated phenotype compared to EV cells. $CD43^+$/ B220+/$CD19^+$ pre-B-cells were more prevalent in EV than hCRLF2 cell populations ($p<0.0008$), suggesting that increased proliferation is accompanied by maintenance of a larger pool of cells with immature immunophenotype: $CD43^+$/ $B220^+$/$CD19^-$ corresponding to Hardy fraction A. (**e**) flow cytometric evaluation of hCRLF2 surface expression in cells from hCRLF2 hematopoietic progenitor colonies at 2^{nd} plating. Solid histogram represents cells stained with a negative control antibody. hCRLF2 positive cells with lower hCRLF2 expression have a higher proportion of $CD43^+$/$CD19^+$ cells (81%) compared to cells with high expression of hCRLF2 (23.5%). By 3^{rd} plating all CRLF2 cells are CD43+/CD19+ with almost negligible μ expression (not shown). (**f**) Cell lysates were prepared from the MUTZ5 cell line, 3 and 4 days following transfection, with either scrambled control (SC), or *CRLF2* shRNA knockdown plasmids (071 and 195) and probed with antibodies specific for CRLF2 or β - actin. (**g**) MUTZ5 cells were transfected with either SC, or *CRLF2* shRNA knockdown plasmid 071 (KD) and proliferation was monitored using an MTS assay (n=3). The down-regulation of *CRLF2* expression in MUTZ5 results in a significant decrease in proliferation ($p=0.0288$, unpaired t-test).

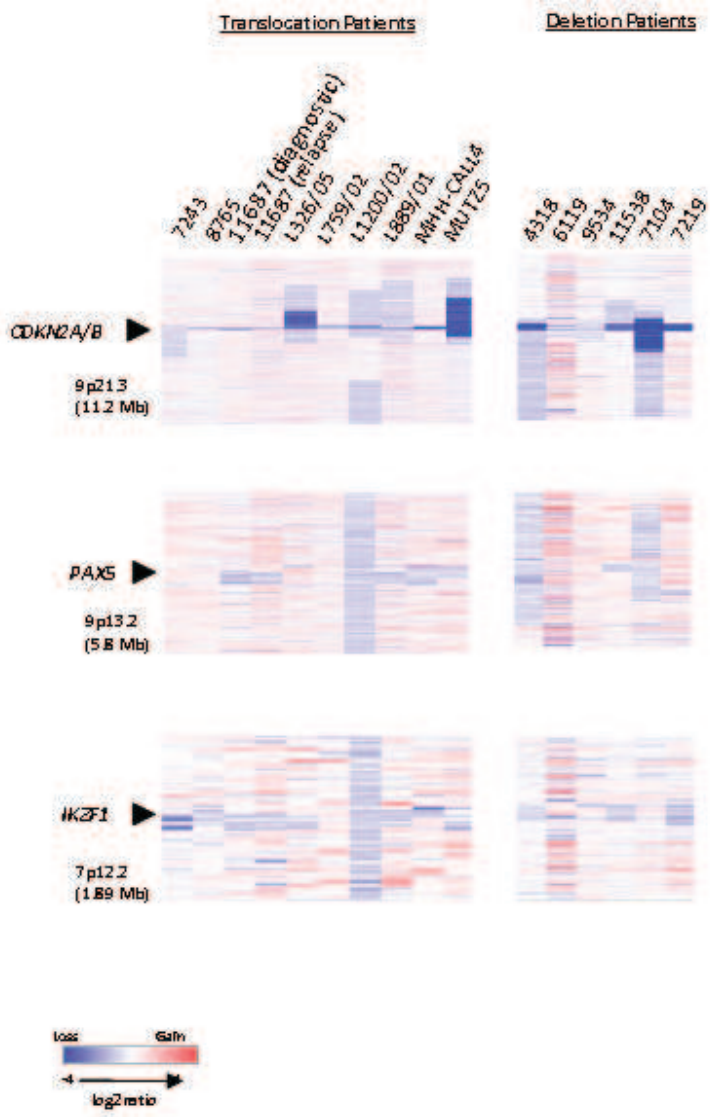
Translocation Patients
Deletion Patients
7243
8765
11687 (diagnostic)
11687 (relapse)
t326/05
t759/02
t1200/02
t869/01
NMH-CALL4
MUTZ5
4318
6119
9534
11538
7104
7219
CDKN2A/B
9p21.3
(11.2 Mb)
PAX5
9p13.2
(5.8 Mb)
IKZF1
7p12.2
(1.89 Mb)
loss
Gain
-1
log2ratio

Figure 4. Heatmaps of 13 diagnostic BCP-ALL samples, 1 relapse and 2 cell-lines. Focal deletions of *CDKN2A/B*, *PAX5* and *IKZF1*. Data are divided by aberration: translocation, t(X;14)(p22;q32) and t(Y;14)(p11;q32), and deletion, del(X)(p22.33p22.33) and del(Y)(p11.32p11.32). For samples with the translocations (7 diagnostic, 1 relapse and 2 cell-lines) data were generated using the Human Genome CGH Microarray 244A platform and for samples with the deletion (6 diagnostic) the Human Genome CGH Microarray 105K platform was used. In all heatmaps each sample is represented by a single column, as indicated by the sample identifier at the head of the figure, and each row denotes the log2ratio for each probe. The probes are plotted in genomic order (hg18) with losses and gains in blue and red. The size of the regions shown are given in parentheses. Note that the additional probes on the Human Genome CGH Microarray 105K platform for the PAR1 region failed.

Supplementary Figure 1: Sequence alignments from all 11 patients and cell lines cloned by LDI-PCR

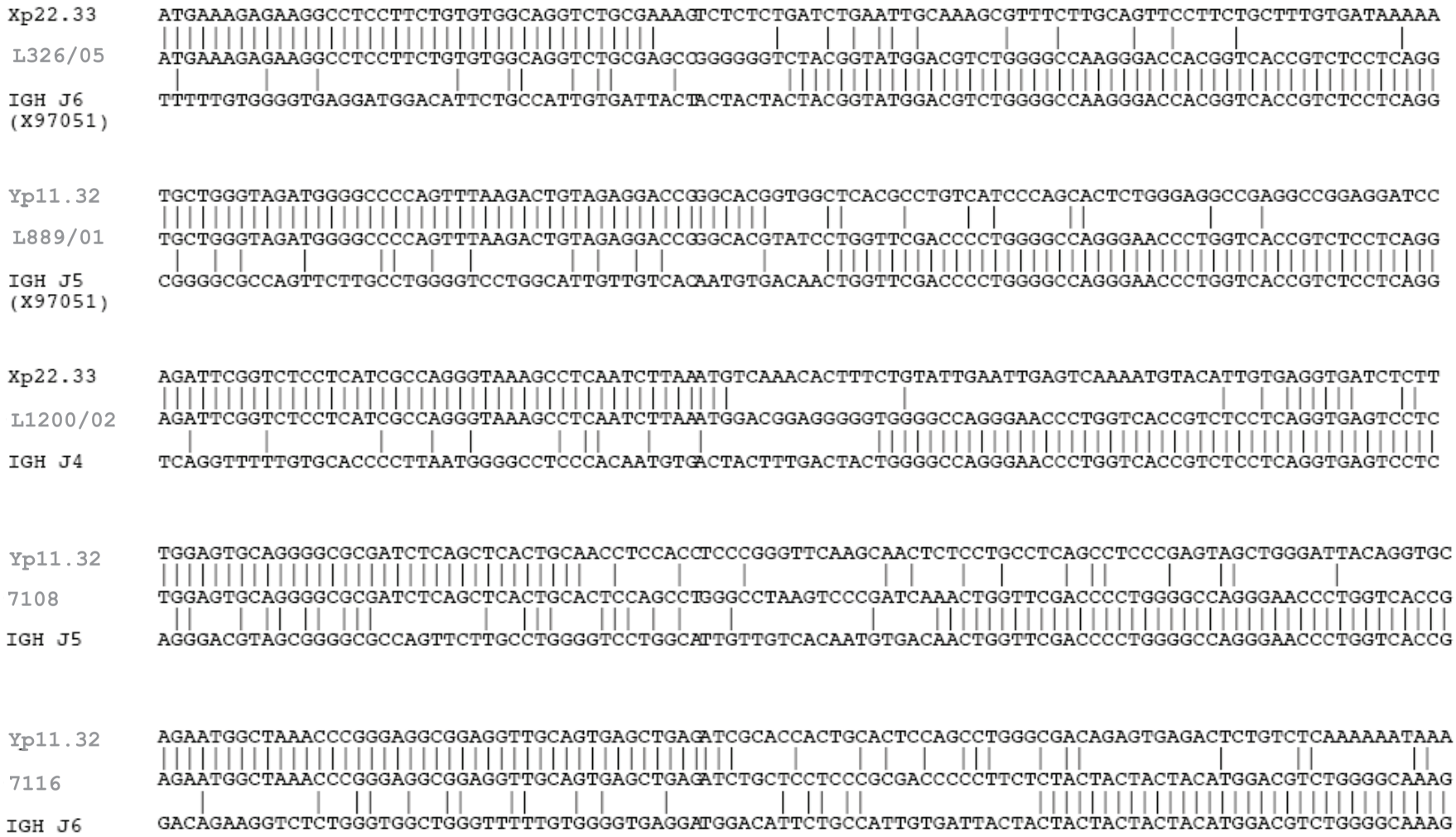

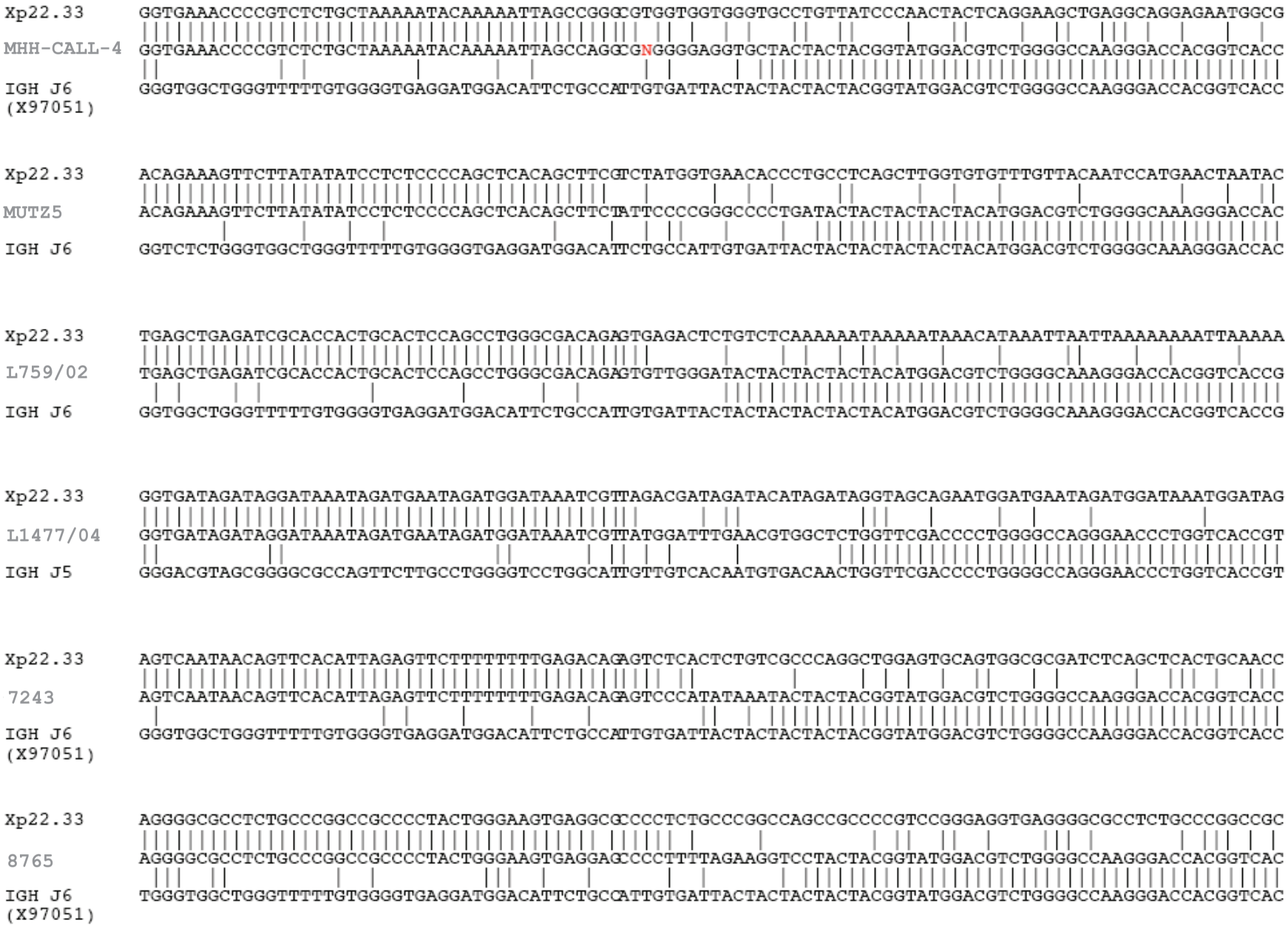
Xp22.33
MHH-CALL-4
IGH J6
(X97051)
Xp22.33
MUTZ5
IGH J6
Xp22.33
L759/02
IGH J6
Xp22.33
L1477/04
IGH J5
Xp22.33
7243
IGH J6
(X97051)
Xp22.33
8765
IGH J6
(X97051)

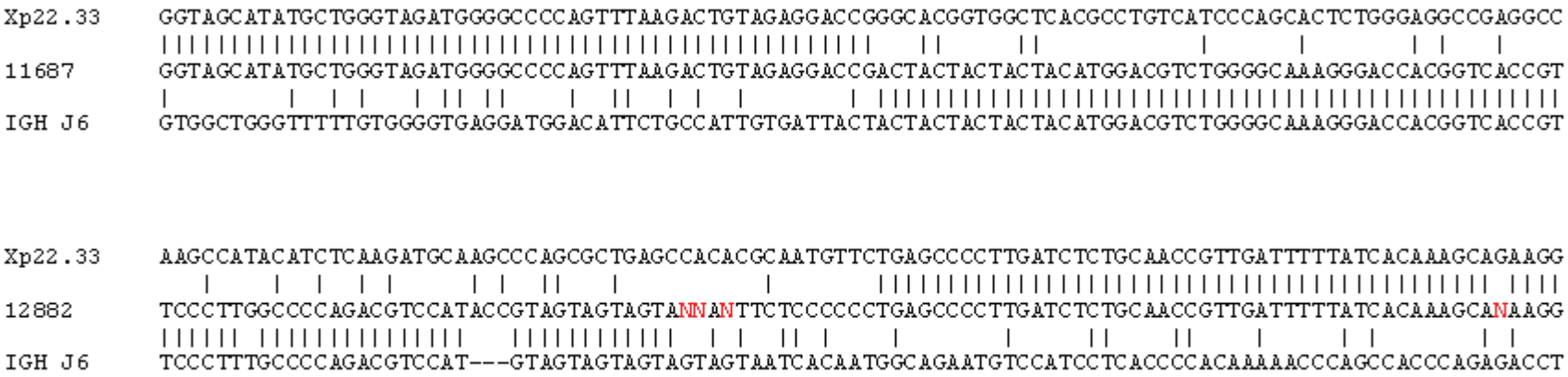
Xp22.33 GGTAGCATATGCTGGGTAGATGGGGCCCCAGTTTAAGACTGTAGAGGACCGGGCACGGTGGCTCACGCCTGTCATCCCAGCACTCTGGGAGGCCGAGGCC
11687 GGTAGCATATGCTGGGTAGATGGGGCCCCAGTTTAAGACTGTAGAGGACCGACTACTACTACTACATGGACGTCTGGGGCAAAGGGACCACGGTCACCGT
IGH J6 GTGGCTGGGTTTTTGTGGGGTGAGGATGGACATTCTGCCATTGTGATTACTACTACTACTACTACATGGACGTCTGGGGCAAAGGGACCACGGTCACCGT
Xp22.33 AAGCCATACATCTCAAGATGCAAGCCCAGCGCTGAGCCACACGCAATGTTCTGAGCCCCTTGATCTCTGCAACCGTTGATTTTTATCACAAAGCAGAAGG
12882 TCCCTTGGCCCCAGACGTCCATACCGTAGTAGTAGTANNANTTCTCCCCCCTGAGCCCCTTGATCTCTGCAACCGTTGATTTTTATCACAAAGCANAAGG
IGH J6 TCCCTTTGCCCCAGACGTCCAT---GTAGTAGTAGTAGTAATCACAATGGCAGAATGTCCATCCTCACCCCACAAAAACCCAGCCACCCAGAGACCT

Supplementary Figure 1 Legend

Sequence alignments to show the location of breakpoints cloned by LDI-PCR from the *IGHJ6* segment. Representative breakpoint sequences with identity to *IGHJ* and the corresponding Xp22.33 or Yp11.32 are shown.

Supplementary Table 1 - Clinical, cytogenetic and genetic results for (a) translocation patients and cell lines; (b) DS ALL and non DS ALL patients with the deletion

(a)

Patient ID	Age (yrs)/Sex	WBC X10^9/L	Karyotype[a]	FISH results				Deletion (D), Translocation (T)	Breakpoint[e]	JAK2 mutations
				IGH@[b]	*CRLF2*[c]	*P2RY8*	*CDKN2A*[d]			
t(X;14)(p22;q32)										
2693	16/F	22	48,X,t(X;14)(p22;q32),+21c,+21[4][f]	1R1G1F (94%)	1R0G1F (71%)	0R1G1F (67%)	NA	D and T	NA	WT[h]
3789	16/F	22	47,X,t(X;14)(p22;q32),+21c[10]	1R1G1F (70%)	1R1G1F (84%)	ND	2R2G (93%)	T	NA	WT[h]
3836	6/F	140	47,X,+X,t(X;14)(p22;q32)[13][f]	1R1G1F (71%) 1R1G1F[i] (26%)	1R1G2F (85%) 1R1G2F[i] (40%)	ND	2R2G (100%) 1R2G[i] (42%)	T	NA	NA
3963	8/F	15	46,X,t(X;14)(p22;q32)[20][f]	1R1G1F (90%)	1R1G1F (93%)	ND	2R2G (97%)	T	NA	NA
4958	4/M	6	48,Y,t(X;14)(p22;q32),+der(X)t(X;14), del(15)(q11.2q15),+21c[2]	1R2G1F (60%)	1R2G1F (54%)	ND	2R2G (96%)	T	NA	R683G[h]
7243	14/M	1	47,Y,t(X;14)(p22;q32),+der(X)t(X;14), der(17)t(9;17)(p1?2;p1?3)[14]	1R2G1F (76%)	1R2G1F (82%)	ND	1R2G (90%)	T	16.2kb centromeric of CRLF2 1,307,705	NA
7389	16/F	105	47,X,+X,t(X;14)(p22;q32),del(6)(q?12q?15), del(9)(p1?3),+21c[3]	1R0G2F (81%) 1R1G1F (12%)	1R0G2F (80%)	0R1G2F (95%)	1R2G (13%)	D and T	NA	WT[h]
8367	30/F	73	46,X,t(X;14)(p22;q32)[22]	1R1G1F (94%)	1R1G1F (86%)	ND	1R2G (90%)	T	NA	NA
8765	5/M	40	47,Y,t(X;14)(p22;q32),+der(X)t(X;14)[6]	1R2G1F (56%) 2R2G0F (25%)	1R2G1F (54%)	ND	2R2G[k] (100%)	T	23.8kb centromeric of CRLF2 1,315,315	NA
10692	3/M	12	49,Y,+X,t(X;14)(p22;q32),+17,+21[5][f]	1R1G1F (72%)	1R0G2F (68%) 1R1G1F (14%)	0R0G2F (96%)	1R2G (61%)	D and T	NA	NA

11687	42/M	280	46,Y,t(X;14)(p22;q32),add(10)(q2?4)[6]	1R1G1F (66%)	1R0G1F (84%)	0R1G1F (94%)	2R2G[k] (99%)	D and T	2.2kb centromeric of *CRLF2* 1,293,751[l]	WT[h]
12882	57/M	36	46,Y,t(X;14)(p22;q32)[10][f]	1R1G1F (73%)	1R1G1F (80%)	ND	NA	T	19.7kb centromeric of *CRLF2* 1,311,210	NA
20033[j]	NA/F	NA	47,X,t(X;14)(p22;q32),+21c[25]	2R1G0F (88%) 2R1G0F[i] (88%)	1R1G1F (94%) 1R1G1F[i] (89%)	ND	2R2G[i] (100%)	T	NA	R683S[h]
21245	17/F	NA	46,X,t(X;14)(p22;q32)[25]	1R1G1F (85%)	1R1G1F (92%)	ND	2R2G (91%)	T	NA	NA
21470	18/M	NA	47,Y,t(X;14)(p22;q32),+der(X)t(X;14)	1R2G1F (79%)	1R2G1F (94%)	ND	2R2G (90%)	T	NA	NA
L326/05	76/F	74	.ish t(X;14)(p22;q32)	1R1G1F (80%)	1R1G1F (33%)	ND	0R2G (58%)	T	19.6kb centromeric of *CRLF2* 1.311,120	NA
L500/06	15/M	NA	47,Y,der(X)t(X;14)(p22;q32),add(7)(p22),add(12)(q24),der(14)t(14;16)(q32;p13),der(16)t(X;14;16)(p22;q32;p13),+21c[cp20]	1R2G1F (80%) 1R1G1F (11%)	0R1G2F	ND	1R2G (7%)	T	NA	WT
L521/06	44/F	NA	.ish t(X;14)(p22;q32)	2R2G0F (67%) 1R1G1F (14%)	1R1G1F (33%) 0R1G2F (18%)	ND	1R2G (10%)	T	NA	NA
L759/02	16/M	24	47,XY,t(X;14)(p22;q32)[5]/48,idem,+X[8]/47,XXYc	1R1G1F (49%)	ND	ND	2R2G[k] (98%)	T	26.9kb centromeric of *CRLF2* 1,318,468	NA
L1138/08	5/M		46,Y,t(X;14)(p22;q32),del(9)(p13p21)[8]	1R1G1F (28%)	1R1G1F (38%)	ND	1R2G (47%)	T	NA	NA
L1200/02	66/F	164	47,X,t(X;14)(p22;q32),+der(X)t(X;14),der(7)del(7)(q11q21)t(7;13)(q21;q12~13),add(9)(p13),der(10)t(?7;10)(q34~35;p13),del(13)(q12~13)[19]	1R2G1F/ 2R2G0F	2R1G1F/ 1R1G1F	ND	1R2G	T	12.4kb centromeric of *CRLF2* 1,303,911	NA
L1477/04	40/M	69	46,Y,t(X;14)(p22;q32),t(5;15)(q23;q21)[3]	2R1G2F	0R1G2F	ND	0R2G (41%)	T	8.5kb centromeric of *CRLF2* 1,300,063	NA

L1796/05	53/F		46,X,t(X;14)(p22;q32)[36]	1R1G1F (50%)	1R1G1F (18%)	ND	2R2G	T	NA	NA
t(Y;14)(p11;q32)										
4001	6/M	9	46,X,t(Y;14)(p11;q32)[30]	1R1G1F (79%)	1R1G1F (89%)	ND	2R2G (97%)	T	NA	NA
7108	48/M	26	46,X,t(Y;14)(p11;q32),del(3)(p2?1)[7]	1R1G1F (73%)	1R0G1F (84%)	NA	2R2G (98%)	D and T	19.9kb centromeric of CRLF2 1,311,386	NA
7114	20/M	342	46,X,t(Y;14)(p11;q32),del(9)(q32q34),del(20)(q1?)[20]	1R1G1F (85%)	1R1G1F (86%)	ND	NA	T	NA	NA
7116	6/M	UK	47,X,t(Y;14)(p11;q32),+21[3]	1R1G1F (84%)	1R1G1F (48%) 1R0G1F (27%)	0R1G1F (12%)	2R2G (99%)	D and T	26.9kb centromeric of CRLF2 1,318,435	NA
7311	10/M	116	46,X,t(Y;14)(p11;q32)[20]	1R1G1F (60%)	1R1G1F (76%)	ND	2R2G (99%)	T	NA	NA
L889/01	40/M	85	46,X,t(Y;14)(p11;q32),-9,del(12)(p11),+mar	1R1G1F (84%)	0R1G2F	ND	1R2G[k] (99%)	T	2.2kb centromeric of *CRLF2* 1,293,757	NA
X/Y unknown										
2326	13/M	90	.nuc ish t(XorY;14)(p22orp11;q32)[g]	NA	1R1G1F (35%)	ND	0R2G (66%)	T	NA	NA
3141	10/M	13	.nuc ish t(X;14)(p22;q32) or t(Y;14)(p11;q32)[g]	NA	1R1G1F (78%)	ND	2R2G (97%) 0R2G[i] (86%)	T	NA	NA
8953	5/M	1	.nuc ish t(X;14)(p22;q32) or t(Y;14)(p11;q32)[g]	1R1G1F (62%)	1R1G1F (66%)	ND	2R2G (100%)	T	NA	NA
9100	46/M	5	.nuc ish t(X;14)(p22;q32) or t(Y;14)(p11;q32)[g]	1R1G1F (13%)	1R1G1F (15%)	ND	2R2G (100%)	T	NA	NA
Cell lines with t(Y;14)(p11;q32)										
MHH-CALL-4	10/M	NA	45,X,-Y,r(12)(p13q24.33),der(14)(t(Y;14)(p11;q32)	1R0G1F (60%)	1R0G1F (97%)	ND	2R2G (97%)	T	2.4kb centromeric of CRLF2 1,293,893	I682F
MUTZ5	26/M	NA	45,X,-Y,t(12;13)(p12;q13~14),der(14)t(Y;14)(p11;q32)	1R0G1F (89%)	1R0G1F (99%)	ND	0R2G (100%)	T	16.1kb centromeric of CRLF2 1,307,580	R683G

(b)

Patient ID	Age	WBC	Karyotype[a]	FISH results					Breakpoint	JAK2

Patient ID	Age (yrs)/Sex	WBC X10^9/L	Karyotype	*IGH@*[l]	*CRLF2*[m]	*P2RY8*[n]	*CDKN2A*		mutations
DS-ALL patients with deletion									
322	4/M	3	48,XY,+X,+21c[5]/49,idem,+17[4]	0R0G2F (99%)	1R0G1F (67%)	0R1G1F (54%)		D	Wt[q]
1655	2/M	9	48,XY,+21c,+21,i(21)(q10)[3]	NA	1R0G1F (78%)	NA		D	NA
1672	7/F	70	47,XX,+21c[20]	NA	1R0G1F (78%) 1R0G2F (26%)	NA		D	NA
2017	1/F	54	47,XX,i(9)(q10),+21c[5]/ 47,idem,del(6)(q13q15)[3]	0R0G2F (97%)	1R0G1F (23%)	NA		D	R683G[q]
3037	2/M	7	46,XY,der(14;21)(q10;q10)c,+21c[18]	0R0G2F (97%)	2R0G1F[p] (68%)	0R2G1F[p] (44%) 0R1G1F (15%)		D	R683G[q]
3410	5/M	53	47,XY,del(9)(p1?3p2?),+21c[10]/ 53,idem,+X,+4,+8,+9,+18,+22[2]	0R0G2F (100%)	1R0G1F (75%)	0R1G1F (57%)		D	R683G[q]
3553	3/F	10	48,XX,+X,+21c,inc[7]	0R0G2F (94%)	2R0G1F (23%)	0R1G2F (42%)		D	R683G[q]
3572	3/M	102	48,XY,+X,t(7;17)(p11;q25),+21c[11]	0R0G2F (96%)	1R0G2F (63%)	NA		D	Failed
4174	2/M	32	47,XY,+21c[18]/46,XY[2]	NA	2R0G1F[p] (88%)	NA		D	Failed
4318	6/M	48	47,XY,del(9)(p22p24),+21c[20]		1R0G1F (92%)	0R1G1F (77%)		D	R683G
4478	4/M	10	47,XY,+9,der(9;16)(q10;p10),+21c[12]	0R0G2F (93%)	1R0G1F (99%)	0R1G1F (73%)		D	R683G[q]
4661	5/F	19	48,XX,+X,+21c[7]	0R0G2F (100%)	2R0G1F (59%)	0R2G1F (81%)		D	Failed
4777	5/M	2	47,XY,+21c[22]	0R0G2F (99%)	1R0G2F[p] (75%) 1R0G1F (9%)	0R1G2F[p] (84%)		D	Wt[q]
4898	3/M	47	47,XY,+21c[10]	0R0G2F (92%)	1R0G1F (84%)	0R1G1F (78%)		D	Failed
5067	3/M	19	47,XY,der(11)t(X;11)(q2?;q2?),+21c[4]/ 47,idem,del(6)(q?)[4]	0R0G2F (90%)	1R0G1F (94%)	0R1G1F (92%)		D	Failed
5762	5/M	3	47,XY,+21c[20]	0R0G2F (98%)	1R0G1F (39%)	0R1G1F (7%)		D	Wt[q]
5817	6/M	69	47,XY,+21c[20]	0R0G2F (91%)	1R0G1F (59%) 2R0G1F[p] (14%)	0R1G1F (55%)		D	NA

6042	2/M	2	48,XY,+Y,+21c[6]	0R0G2F (99%)	2R0G1F (74%)	0R2G1F (80%) 0R2G1F (11%)	D	Failed
6119	3/M	9	50,XY,+X,+Y,+21c,+21[17]	0R0G2F (97%)	2R0G2F (71%)	0R2G2F (80%) 0R1G2F (31%)	D	R683G
6997	2/M	NA	47,XY,+21c	0R0G2F (99%)	1R0G2F[p] (55%)	0R1G2F[p] (88%)	D	NA
7191	8/M	80	47,XY,+21c	0R0G2F (95%)	1R0G1F (89%)	0R1G1F (97%)	D	Failed
7643	3/M	83	47,XY,del(12)(p11.1),+21c[5]	0R0G2F (96%)	1R0G1F (69%)	0R1G1F (77%)	D	NA
7761	3/M	48	47,XY,+21c[20]	0R0G2F (100%)	1R0G1F (12%) 2R0G1F[p] (83%)	0R2G1F[p] (94%)	D	Failed
8274	2/F	8	47,XX,+21c[13]	0R0G2F (99%)	1R0G1F (83%)	0R1G1F (72%)	D	NA
9534	2/M	65	47,XY,+21c[20]	0R0G2F (96%)	1R0G1F (96%)	0R1G1F (95%)	D	NA
10607	4/M	25	48,XY,+X,del(1)(q32),+21c[6]/ 48,XY,+X,add(1)(q32),+21c[3]	0R0G2F (96%)	2R0G1F (74%)	0R2G1F (97%)	D	NA
10841	3/M	24	47,XY,+21c[14]	0R0G2F (100%)	1R0G1F (89%)	0R1G1F (85%)	D	NA
10924	2/M	23	47,XY,+21c[20]	0R0G2F (99%)	1R0G2F (79%)	0R1G2F (95%)	D	Failed
11101	3/F	4	47,XX,add(19)(p13.3),+21c[8]	0R0G2F (99%)	1R0G1F (71%) 1R0G2F[p] (12%)	0R1G1F (75%) 0G1R2F[p] (7%)	D	NA
11463	3/F	103	47,XX,+21c[2]	0R0G2F (95%)	1R0G1F (46%)	0R1G1F (81%)	D	R683S
11538	8/M	400	47,XY,-2,add(14)(q32),+21c,+mar[5]	NA	1R0G1F (91%)	NA	D	NA
11734	8/F	12	47,XX,+21c[20]	0R0G2F (100%)	1R0G1F (31%)	0R1G1F (64%)	D	NA
12200	3/M	96	49,XY,+X,+9,add(12)(p1?),+21c[12]	0R0G2F (100%)	1R0G2F (72%)	0G1R2F (77%) 0R1G1F (7%)	D	R683 mutation[r]
20449	4/M	30	47,XY,+21c[25]	0R0G2F (96%)	1R0G1F (90%)	0R1G1F (77%)	D	NA
20638	4/F	5	47,XX,+21c[20]	0R0G2F (100%)	1R0G1F (47%)	0R1G1F (38%)	D	NA
Non-DS-ALL patients with deletion							D	

2904[s]	15/F	1	46,XX,del(7)(q22q32),dup(21)(q?)[16]	0R0G2F (97%)	1R0G1F (75%)	0R1G1F (62%)	D	NA
2964	4/M	7	47,XY,+17[5]	0R0G2F (100%)	1R0G1F (90%)	0R1G1F (80%)	D	NA
2966	3/F	70	47-48,XX,+17,del(20)(?p/q),+21,+mars,inc[cp9]/46,XX,del(7)(p11)[8]	0R0G2F (99%)	1R0G1F (94%)	0R1G1F (92%)	D	NA
2977	12/F	2	51,XX,+X,+X,+4,+21,+21[20]	0R0G2F (93%)	1R0G3F (89%)	0R1G3F (96%)	D	NA
3173	3/M	5	50,XY,+X,+9,+14,+21[14]	0R0G3F (55%) 0R0G2F (39%)	2R0G1F (65%)	0R2G1F (69%)	D	NA
3368[s]	20/M	6	46,XY,del(7)(p1?5),t(8;22)(q1?1;q13),dup(21)(q?)[17]	0R0G2F (99%)	1R0G1F (95%)	0R1G1F (97%)	D	NA
3396	6/F	3	46,XX,der(2)t(X;2)(q?;q35),i(7)(q10)[3]	0R0G2F (93%)	1R0G1F (90%)	0R1G1F (85%)	D	NA
3450	2/M	32	45,XY,dic(9;20)(p11~13;q11)[13]	0R0G2F (99%)	1R0G1F (49%)	0R1G1F [50%)	D	NA
4002	1/F	131	46,XX[10]	0R0G2F (98%)	1R0G1F (84%)	0R1G1F (84%)	D	NA
4184	7/M	135	25<1n>,XY,+21[9]/50,idem x2[3]	0R0G1F (68%) 0R0G2F (29%)	1R0G1F (81%)	0R1G1F (66%)	D	NA
4247	4/F	31	46,XX,add(21)(q22)[23]	0R0G2F (93%)	1R0G1F (96%)	0R1G1F (92%)	D	NA
4316[s]	5/F	22	46,XX[24]	0R0G2F (93%)	1R0G1F (43%)	NA	D	NA
4422	3/F	119	Fail	0R0G2F (97%)	2R0G1F[p] (37%)	0R2G1F[p] (52%)	D	NA
4451	2/F	22	45,XX,dic(9;20)(p11~13;q11),del(16)(q22)[2]	0R0G2F (96%)	1R0G1F (95%)	0R1G1F (94%)	D	NA
4561[s]	9/M	4	Fail	0R0G2F (93%)	2R0G2F[p] (92%)	0R2G2F[p] (95%)	D	NA
4623[s]	6/F	14	46,XX,dup(21)(q?)[11]/47,idem,+X[1]	0R0G2F (93%)	1R0G1F (86%)	0R1G1F (87%)	D	NA
4640	3/M	6	55-56,XY,+X,+4,+8,+10,+14,+add(18)(q23),+19,+21,+21,+21[cp4]	0R0G3F (86%) 0R0G2F (11%)	2R0G3F[p] (72%)	0R2G3F[p] (89%) 0R1G2F[p] (7%)	D	NA
4785	1/F	2	49,XX,+X,+X,+21[7]	0R0G2F (92%)	2R0G2F (81%) 1R0G2F (14%)	0R2G2F (92%)	D	NA
4792	3/F	6	47,XX,+X[3]	0R0G2F (96%)	2R0G1F (76%)	0R2G1F (70%)	D	NA

5655[s]	8/F	55	46,XX,del(1)(q4?),del(6)(q1?5),del(7)(q2?2q3?1),dup(21)(q?)[3]/ 46,idem,add(6)(q2?)[12]	0R0G2F (97%)	1R0G1F (95%)	0R1G1F (93%)	D	NA
5674[s]	6/M	55	47,XY,+X,dup(21)(q?)[7]	0R0G2F (98%)	2R0G1F (84%)	0R2G1F (83%) 0R1G1F (7%)	D	NA
6814	1/M	29	46,XY[20]	0R0G2F (98%)	1R0G1F (83%)	0R1G1F (79%)	D	NA
6915	8/F	16	47,XX,+X[7]	0R0G2F (98%)	1R0G2F (70%)	0R1G2F (67%) 0R1G3F[p] (9%)	D	NA
6937[s]	6/F	85	46,XX,dup(21)(q?)[10]	0R0G2F (99%)	1R0G1F (100%)	0R1G1F (92%)	D	NA
7015	2/F	UK	47,XX,+X,t(2;14)(p1?1;q11),-7, i(21)(q10)x2,+mar	0R0G2F (99%)	2R0G1F (80%) 1R0G1F (11%)	0R1G2F (83%)	D	NA
7104	35/M	20	47,XY,+X,t(9;15)(p?1;q?1)[20]	0R0G2F (95%)	1R0G2F (87%)	0R1G2F (85%)	D	NA
7219[s]	15/M	2	46,XY,der(21)dup(21)(q?),inc[3]	0R0G2F (92%)	1R0G1F (49%)	0R1G1F (34%)	D	NA
7583[s]	14/M	3	47,XY,+X,der(21)r(21)(q?)dup(21)(q?)[4]	0R0G2F (98%)	1R0G2F (95%)	0R1G2F (85%)	D	NA
8767[s]	10/F	130	46,XX[8]	0R0G2F (99%)	1R0G1F (94%)	0R1G1F (97%)	D	NA

Supplementary Table 1 legend

[a]Karyotypes are described according to ISCN (2005)[1]. Normal clones have been omitted from abnormal karyotypes.

[b]All patients had a positive result with the *IGH*@ probe indicating the presence of a translocation, percentage of positive cells was variable. Percentages are not provided when less than 100 cells were available for analysis.

[c]All patients showed a positive result with the *CRLF2* specific probes indicating involvement of either Xp22 or Yp11 in the translocation. Percentages (where given) are variable. The signal patterns indicate the presence of an additional normal or derived X chromosome and deletions associated with the translocation.

[d]Deletions of *CDKN2A* were identified by FISH as monoalleleic (1R2G) or biallelic (0R2G). Percentages (where given) are variable.

[e]BLAT search results using March 2006 assembly (http://genome.ucsc.edu/cgi-bin/hgBlat?command=start).

D; deletion present

T; translocation present

ND; Not done.

NA; Not available.

[f]Cryptic t(X;14) not seen on metaphase but inferred from positive interphase FISH results.

[g]In these male patients it is unknown whether the translocation affects the X or Y chromosome.

[h]Previously reported[2].

[i]Present in relapse sample.

[j]Karyotype from relapse sample. Translocation seen by FISH at both diagnosis and relapse, however *JAK2* mutation seen only in relapse sample.

[k]Biallelic deletion detected by aCGH.

[l]Patients had a normal result with the *IGH*@ probe indicating the absence of a translocation.

[m]All patients showed the loss of a green signal with the *CRLF2* probe 1 indicating the presence of a deletion centromeric of *CRLF2 .*

[n]Loss of the red signal indicates that the deletion covers the telomeric region of *P2RY8*.

[p]FISH patterns for *CRLF2* and *P2RY8* suggest the presence of additional sex chromosome(s) not seen by convention cytogenetics.

[q]Previously reported[2]

[r]Complex mutation - L681-I682insRGV

[s]Patient has karyotype with intrachromosomal amplification of chromosome 21 (iAMP21).

1. Schafer, L. & Tommerup, N. *An International System for Human Cytogenetic Nomenclature*, 1-130 (S.Karger, Basel, 2005).
2. Kearney, L. et al. A specific JAK2 mutation (JAK2R683) and multiple gene deletions in Down syndrome acute lymphoblastic leukaemia. *Blood*, blood-2008-08-170928 (2008).

Supplementary Table 2: Summary of breakpoints cloned by LDI-PCR

Patient ID	Age/Sex	Location of PAR1 breakpoint and distance from *CRLF2*	Breakpoint on IGH
11687	42/M	2.2kb centromeric of *CRLF2* 1,293,751	IGHJ6
L889/01	40/M	2.2kb centromeric of *CRLF2* 1,293,757	IGHJ5
MHH-CALL-4	10/M	2.4kb centromeric of *CRLF2* 1,293,893	IGHJ6
L1477/04	40/M	8.5kb centromeric of *CRLF2* 1,300,063	IGHJ5
L1200/02	66/F	12.4kb centromeric of *CRLF2* 1,303,911	IGHJ4
MUTZ5	26/M	16.1kb centromeric of *CRLF2* 1,307,580	IGHJ6
7243	14/M	16.2kb centromeric of *CRLF2* 1,307,705	Between IGHJ6 and IGHM
L326/05	76/F	19.6kb centromeric of *CRLF2* 1.311,120	IGHJ6
12882	57/M	19.7kb centromeric of *CRLF2* 1,311,210	IGHJ6
7108	48/M	19.9kb centromeric of *CRLF2* 1,311,386	IGHJ5
8765	5/M	23.8kb centromeric of *CRLF2* 1,315,315	Between IGHJ6 and IGHM
7116	6/M	26.9kb centromeric of *CRLF2* 1,318,435	IGHJ6
L759/02	16/M	26.9kb centromeric of *CRLF2* 1,318,468	IGHJ6

Supplementary Table 3: aCGH data summary

Sample	Chromosome	Aberration	Size (Mb)	Start	End	Key Genes
Translocation Patients						
7243	4	deletion	0.75	68896316	69643331	UGT2B17
7243	7	deletion	0.09	38281765	38372751	TRG@7p14.1
7243	7	deletion	0.08	50378518	50461374	IKZF1
7243	9	deletion	2.53	21904800	24439398	MTAP, CDKN2A, CDKN2B, DMRTA1, ELVAL2
7243	9	deletion	0.13	37200772	37331060	ZCCHC7
7243	12	deletion	4.24	123344064	127581807	NCOR2, SCARB1, DHX37
7243	12	deletion	2.24	128845604	131088241	RIMBP2, STX2, GPR133
7243	14	deletion	0.14	21944246	22081151	TRA@14q11.2
7243	14	deletion	0.06	105391340	105455843	IGH@14q32.33
7243	17	deletion	18.79	76263	18869125	SLC43A2, GARNL4, UBE2G1, SLC16A11, TP53, PIK3R5, GAS7, MAP2K4, COX10, SLC5A1(
7243	17	gain	0.69	68069331	68755768	SLC39A11
7243	22	deletion	0.23	20847633	21075427	IGL@22q11.2
7243	22	deletion	0.08	23973040	24056409	CRYBB2
7243	X	gain	154.91	1	154913754	Gain of whole chromosome
8765	1	deletion	0.12	246755225	246875051	OR2T10
8765	2	deletion	0.68	88692777	89377632	IGK@2p11.2
8765	3	deletion	0.15	196822133	196968303	MUC20
8765	6	deletion	0.75	88355973	89106207	ORC3L, C6orf166, SPAC1, CNR1
8765	7	deletion	0.14	50303641	50440071	IKZF1
8765	8	deletion	0.19	39341524	39535714	ADAM5P
8765	9	deletion	0.11	21910518	22018332	CDKN2A, CDKN2B
8765	10	gain	1.53	45491659	47026056	PPYR1
8765	11	deletion	0.11	55118214	55225195	OR4P4
8765	14	deletion	19.84	2198644	22034762	TRA@14q11.2
8765	14	deletion	0.05	105845658	105898731	IGH@14q32.33
8765	14	deletion	0.07	105946993	106017512	IGH@14q32.33
8765	22	deletion	0.20	20797302	20999525	IGL@22q11.2
8765	22	deletion	0.25	47650278	47899993	no known genes
8765	X	gain	154.91	1	154913754	Gain of whole chromosome
11687 (Diagnostic)	1	deletion	0.24	92301285	92545386	C1orf146, GLMN
11687 (Diagnostic)	2	deletion	0.14	54628305	54769860	SPTBN1
11687 (Diagnostic)	2	deletion	0.40	57838960	58237651	VRK2
11687 (Diagnostic)	2	deletion	0.47	88932397	89400147	IGK@2p11.2
11687 (Diagnostic)	3	deletion	0.53	22694449	23225331	no known genes
11687 (Diagnostic)	3	deletion	0.12	35625741	35743651	ARPP-21
11687 (Diagnostic)	3	deletion	1.56	59957537	61516874	FHIT
11687 (Diagnostic)	3	deletion	0.19	113522351	113707527	BTLA, ATG3
11687 (Diagnostic)	4	deletion	0.11	86710860	86823631	ARHGAP24
11687 (Diagnostic)	4	deletion	0.54	149576081	150112334	no known genes
11687 (Diagnostic)	6	deletion	0.26	26388786	26647186	BTN2A2, BTN3A1
11687 (Diagnostic)	6	deletion	0.13	32558677	32684017	HLA-DRB5
11687 (Diagnostic)	6	deletion	0.21	109236068	109441635	ARMC2
11687 (Diagnostic)	7	deletion	0.11	38259147	38372751	TRG@7p14.1
11687 (Diagnostic)	7	deletion	0.69	50010718	50700575	IKZF1
11687 (Diagnostic)	7	deletion	0.19	142021348	142212407	TRB@7q34
11687 (Diagnostic)	8	deletion	0.14	22398397	22539377	PPP3CC, SORBS3, PDLIM2, BIN3
11687 (Diagnostic)	8	gain	0.21	39302253	39511632	ADAM5P
11687 (Diagnostic)	8	deletion	0.13	135791049	135917097	ZFAT
11687 (Diagnostic)	9	deletion	0.70	1997646	2701245	SMARCA2, VLDLR
11687 (Diagnostic)	9	deletion	0.05	21947735	21999029	CDKN2A, CDKN2B
11687 (Diagnostic)	9	deletion	0.31	36996073	37310759	PAX5, ZCCHC7
11687 (Diagnostic)	9	deletion	0.34	83475009	83814745	FLJ46321
11687 (Diagnostic)	10	deletion	8.21	127071459	135286082	FANK1, ADAM12, DOCK1, PTPRE, MGMT, EBF3, INPP5A, KNDC1
11687 (Diagnostic)	11	deletion	0.08	55118214	55200803	OR4P4
11687 (Diagnostic)	12	deletion	0.31	90772718	91083040	BTG1
11687 (Diagnostic)	14	gain	1.37	18149473	19515840	A26C2, olfactory gene cluster
11687 (Diagnostic)	14	deletion	0.39	21682650	22071839	TRA@14q11.2

11687 (Diagnostic)	14	deletion	0.93	105422205	106349815	IGH@14q32.33
11687 (Diagnostic)	15	deletion	0.22	48367835	48590023	USP8
11687 (Diagnostic)	22	deletion	0.58	20707320	21284931	IGL@22q11.2
11687 (Diagnostic)	X	deletion	0.28	41726185	42005101	no known genes
11687 (Diagnostic)	X	gain	57.50	97083641	154582473	From DIAPH2 to telomere
11687 (Relapse)	1	deletion	0.24	92301285	92545386	BTBD8, C1orf46, GLMN
11687 (Relapse)	2	deletion	0.74	88932397	89669546	IGK@2p11.2
11687 (Relapse)	3	deletion	0.17	35625741	35797077	ARPP-21
11687 (Relapse)	3	deletion	1.34	60030517	61372165	FHIT
11687 (Relapse)	4	deletion	0.13	86705507	86839419	ARHGAP24
11687 (Relapse)	6	deletion	0.27	26381558	26647245	Butyrophilin gene cluster within MHC regior
11687 (Relapse)	7	deletion	0.11	38270942	38380392	TRG@7p14.1
11687 (Relapse)	7	deletion	0.13	50332222	50461315	IKZF1
11687 (Relapse)	7	deletion	0.19	142021348	142212407	TRB@7q34
11687 (Relapse)	9	deletion	0.05	21947735	21999029	CDKN2A, CDKN2B
11687 (Relapse)	9	deletion	0.31	36970017	37275999	PAX5, ZCCHC7
11687 (Relapse)	10	deletion	8.36	126925052	135286082	FANK1, ADAM12, DOCK1, MGMT, EBF3, TCERG1L, BNIP3, INPP5A, MTG1
11687 (Relapse)	12	deletion	0.40	90744300	91141144	BTG1
11687 (Relapse)	14	deletion	0.08	21958644	22034762	TRA@14q11.2
11687 (Relapse)	14	deletion	0.89	105455799	106349815	IGH@14q32.33
11687 (Relapse)	22	deletion	0.28	20714751	20999525	IGL@22q11.2
11687 (Relapse)	X	deletion	0.34	41669989	42005101	no known genes
11687 (Relapse)	X	gain	57.25	97146509	154396953	From DIAPH2 to telomere
L326/05	2	deletion	2.13	88924973	91057181	IGK@2p11.2
L326/05	3	deletion	0.00	47039911	47039970	SETD2
L326/05	5	deletion	0.41	71441440	71848880	MAP1B, MRPS27, PTCD2, ZNF366
L326/05	6	deletion	0.00	15325879	15325938	JARID2
L326/05	6	deletion	0.27	26380732	26652352	Butyrophilin gene cluster in MHC regior
L326/05	7	deletion	0.10	38244071	38347880	TRG@7p14.1
L326/05	7	deletion	0.14	50378518	50513704	IKZF1
L326/05	7	deletion	0.23	141978682	142207206	TRB@7q34
L326/05	8	deletion	0.15	39363050	39511691	ADAM5P
L326/05	9	deletion	2.97	20344847	23316798	MLLT3, KIAA1797, with homozygous deletion from 21,294,530 to 21,904,859 bp including MTAP, CDKN2A and CDKN2E
L326/05	11	deletion	2.23	89098815	91328760	PSMAL, NAALAD2
L326/05	11	deletion	1.18	91952982	93130184	FAT3, SLC36A4, CCDC67, C11orf75
L326/05	11	deletion	1.98	95983844	97961158	no known genes
L326/05	11	deletion	4.40	107905113	112309006	KDELC2, EXPH5, DDX10, FDX1, ARHGAP20, BTG4, SNF1LK2, DIXDC1, DLAT, NCAM1
L326/05	11	deletion	0.31	112940396	113246813	TMPRSS5, ZW10, USP28
L326/05	12	deletion	47.66	149697	47809829	HDAC7, VDR, COL2A1, CCNT1, DDX23, RND1, ARF3, WNT10B, MLL2
L326/05	13	deletion	0.12	47872085	47987537	RB1
L326/05	14	gain	1.39	18149532	19535787	Olfactory gene cluster
L326/05	14	deletion	0.40	21682650	22081151	TRA@14q11.2
L326/05	14	deletion	0.05	105398979	105447413	IGH@14q32.33
L326/05	14	deletion	0.23	105898674	106125384	IGH@14q32.33
L326/05	18	deletion	0.13	72989670	73116064	GALR1
L326/05	22	deletion	0.22	20714751	20929852	IGL@22q11.2
L759/02	2	deletion	0.15	88924973	89078653	IGK@2p11.2
L759/02	5	deletion	0.09	745859	837297	no known genes
L759/02	7	deletion	0.09	38259147	38347880	TRG@7p14.1
L759/02	9	deletion	0.17	21827873	21998655	MTAP, CDKN2A, CDKN2B
L759/02	14	deletion	1.35	18149473	19497082	Olfactory receptor gene cluster
L759/02	14	deletion	0.37	21698018	22071839	TRA@14q11.2
L759/02	14	deletion	0.14	36856592	36992859	MIPOL1
L759/02	14	deletion	1.00	105330913	106334523	IGH@14q32.33
L759/02	16	gain	0.25	72645154	72893640	PSMD7
L759/02	X	gain	154.91	1	154913754	Gain of whole chromosome
L1200/02	2	deletion	0.84	88910647	89750203	IGK@2p11.2
L1200/02	3	deletion	0.21	163912209	164123865	no known genes
L1200/02	4	deletion	0.74	68905670	69643331	UGT2B17

L1200/02	6	gain	0.16	32519935	32684017	HLA-DRB5
L1200/02	7	deletion	3.61	5831281	9439339	EIF2AK1, USP42, PSCD3, RAC1, DAGLB, COL28A1, RPA3, GLCCI1, ICA1, NXPH1
L1200/02	7	deletion	2.95	9756755	12704296	PHF14, THSD7A, SCIN
L1200/02	7	deletion	20.26	36330467	56593841	ELMO1, EPDR1, POU6F2, GLI3, HECW1, URG4, NUDCD3, CCM2, IKZF1 and TRG@7p14.1
L1200/02	7	deletion	1.43	87918996	89348062	ZNF804B
L1200/02	7	deletion	0.12	129403802	129522219	ZC3HC1
L1200/02	8	deletion	0.00	39363050	39363109	ADAM5P
L1200/02	9	deletion	3.51	6684944	10196477	JMJD2C, PTPRD
L1200/02	9	deletion	2.20	20510469	22712685	MLLT3, KIAA1797, MTAP, CDKN2A, CDKN2B, DMRTA1 with homozygous deletion from 21,862,531 to 21,958,041 b
L1200/02	9	deletion	12.21	26918356	39131894	TEK, MOBKL2B, LINGO2, ACO1, DDX58, B4GALT1, NFX1, UNC13B, PAX5, ZCCHC7, IGFBPL1
L1200/02	10	deletion	3.86	25558239	29420226	GPR158, MYO3A, GAD2, APBB1IP, PTCHD3, MKX, MPP7, WAC
L1200/02	13	deletion	4.61	28841482	33455557	SLC7A1, B3GALTL, RXFP2, FRY, STARD13,
L1200/02	13	deletion	0.12	47862424	47978526	RB1
L1200/02	14	deletion	0.15	21931667	22081151	TRA@14q11.2
L1200/02	14	deletion	0.15	105391340	105545604	IGH@14q32.33
L1200/02	15	gain	2.03	18362555	20393645	LOC283755, A26B1
L1200/02	17	gain	0.53	41521544	42049599	KIAA1267
L1200/02	22	deletion	0.19	20707320	20899881	IGL@22q11.2
L1200/02	X	gain	154.91	1	154913754	Gain of whole chromosome
L889/01	2	deletion	0.45	88955127	89401892	IGK@2p11.2
L889/01	3	deletion	0.10	164023502	164123865	no known genes
L889/01	5	deletion	1.40	28981864	30385790	no known genes
L889/01	6	deletion	1.15	155647935	156793024	NOX3
L889/01	7	deletion	0.05	38281765	38336023	TRG@7p14.1
L889/01	7	deletion	0.14	50323608	50461315	IKZF1
L889/01	8	deletion	0.15	39363050	39511691	ADAM5P
L889/01	9	deletion	3.81	19956040	23761325	MLLT3, KIAA1797, MTAP with a region of homozygous deletion from 21,934,037 to 22,115,464 bp involving CDKN2A and CDKN2I
L889/01	9	deletion	0.31	37011020	37317830	PAX5, ZCCHC7
L889/01	13	deletion	0.11	40040679	40147070	FOXO1
L889/01	14	deletion	0.08	21944246	22022119	TRA@14q11.2
L889/01	14	deletion	0.27	105398979	105672674	IGH@14q32.33
L889/01	22	deletion	0.30	20707320	21005035	IGL@22q11.2
MHH-CALL-4	2	deletion	0.85	88903639	89750203	IGK@2p11.2
MHH-CALL-4	4	deletion	0.19	70108511	70299604	UGT2B11, UGT2B28
MHH-CALL-4	6	deletion	0.64	149384247	150024761	MAP3K7IP2, ZC3H12D, PPIL4, KATNA1
MHH-CALL-4	7	deletion	0.06	38281765	38343085	TRG@7p14.1
MHH-CALL-4	7	deletion	0.09	50316797	50411763	IKZF1
MHH-CALL-4	7	deletion	0.28	141928581	142207206	TRB@7q34
MHH-CALL-4	9	deletion	0.20	21795270	21998655	CDKN2A, CDKN2B
MHH-CALL-4	9	deletion	0.40	36894709	37295552	PAX5, ZCCHC7
MHH-CALL-4	12	deletion	4.65	9116339	13764759	IQSEC3, SL6A12, ERC1, CACNA1C, PRMT8, A2ML1, A2M, STYK1, PRR4, ETV6, EMP1
MHH-CALL-4	14	deletion	0.80	21342040	22142192	TRA@14q11.2
MHH-CALL-4	14	deletion	0.97	105379293	106349815	IGH@14q32.33
MHH-CALL-4	18	deletion	0.31	30769171	31080591	MAPRE2
MHH-CALL-4	18	deletion	0.30	71769299	72070913	no known genes
MHH-CALL-4	22	deletion	0.19	20678912	20870891	IGL@22q11.2
MHH-CALL-4	Y	deletion	57.77	1	57772954	Whole chromosome loss
MUTZ5	1	deletion	0.10	44661637	44761066	C1orf164
MUTZ5	1	deletion	1.04	166600878	167643338	XCL1, DPT, ATP1B1, NME7
MUTZ5	2	deletion	1.19	31362637	32548782	XDH, SRD5A2, MEMO1, DPY30, SPAST, SLC30A6, NLRC4, BIRC6
MUTZ5	2	deletion	0.42	88966417	89387655	IGK@2p11.2
MUTZ5	3	deletion	4.00	28972234	32970637	RBMS3, TGFBR2, GADL1, STT3B, OSBPL10, GPD1L, CMTM6-8, DYNC1LI1, CNOT10, TRIM7
MUTZ5	4	deletion	0.05	109201957	109249314	LEF1
MUTZ5	5	gain	0.14	40782390	40925748	CARD6
MUTZ5	6	deletion	0.76	25948251	26706335	SLC17A2, TRIM38, Histones
MUTZ5	7	deletion	0.07	38270942	38343085	TRG@7p14.1
MUTZ5	7	deletion	0.08	50378518	50461374	IKZF1
MUTZ5	7	deletion	0.45	106652033	107106312	COG5
MUTZ5	8	gain	0.13	39368509	39493946	ADAM5P

MUTZ5	9	deletion	3.76	19716199	23476509	MLLT3, KIAA1797, with homozygous deletion from 20,810,273 to 22,712,626 bp including KIAA1797, MTAP, CDKN2A, CDKN2E
MUTZ5	9	deletion	0.16	36914227	37077995	PAX5, ZCCHC7
MUTZ5	10	gain	0.11	46408696	46520450	PYPR1
MUTZ5	11	deletion	0.08	55118214	55200803	Olfactory receptor gene cluster
MUTZ5	11	deletion	3.40	60479967	63883940	CD6, DDB1, DAK, INCENP, STX5, SLC3A2, MARK2, MACROD1, VEGFE
MUTZ5	12	deletion	1.95	10474925	12422188	STYK1, PRR4, with homozygous deletion from 11,444,721 to 12,265,365 bp involving ETV6 and BCL2L14
MUTZ5	12	deletion	0.30	90772718	91072424	BTG1
MUTZ5	13	deletion	0.52	19676847	20198651	CRYL1
MUTZ5	13	deletion	0.00	43742482	43742541	SERP2
MUTZ5	13	deletion	0.31	47845532	48154217	RB1, RCBTB2
MUTZ5	13	deletion	2.35	48969312	51319974	EBPL, KPNA3, DLEU7, INTS6, WDFY2
MUTZ5	14	deletion	0.15	21920051	22066201	TRA@14q11.2
MUTZ5	14	deletion	0.59	105693581	106280474	IGH@14q32.33
MUTZ5	15	gain	1.91	18454050	20366729	LOC283755, A26B1
MUTZ5	15	deletion	0.14	23523883	23660271	ATP10A
MUTZ5	17	deletion	1.02	47257983	48275965	CA10
MUTZ5	19	deletion	0.69	1749246	2434846	SCAMP4, BTBD2, SPPL2B, TMPRSS9
MUTZ5	20	deletion	0.00	1506379	1506438	SIRPB1
MUTZ5	20	deletion	0.08	10360303	10437156	C20orf94
MUTZ5	22	deletion	0.19	20701592	20886733	IGL@22q11.2
MUTZ5	22	deletion	0.33	21255062	21588229	IGL@22q11.2
MUTZ5	22	deletion	0.07	22656831	22731242	GSTT1
MUTZ5	X	deletion	1.05	44132095	45183894	FUNDC1, DUSP21, UTX, CXorf36
MUTZ5	Y	deletion	57.77	1	57772954	Whole chromosome loss
Deletion Patients						
4318	2	deletion	2.18	88857041	91034025	IGK@2p11.2
4318	6	deletion	0.17	32520387	32689774	HLA-DRB1
4318	7	deletion	0.10	50334299	50432810	IKZF1
4318	8	deletion	0.24	39341523	39586202	ADAM5P
4318	9	deletion	17.40	21733409	39130221	Includes homozgous deletions from 21,963,069 to 21,998,981 bp involving CDKN2A/B and from 36,907,113 to 36,982,704 bp PAX5
4318	12	deletion	0.19	63748913	63938767	WIF1, LEMD3
4318	14	deletion	0.67	21412147	22086378	TRA@14q11.2
4318	14	deletion	0.99	105322190	106311854	IGH@14q32.33
4318	15	gain	1.48	18741715	20220415	Immuloglobulin heavy chain VHDJ mRNAs
4318	21	gain	46.94	1	46944323	Whole chromosome gain
4318	22	deletion	0.29	20707319	20999465	IGL@22q11.2
6119	2	deletion	0.46	88924972	89387595	IGK@2p11.2
6119	3	deletion	0.33	163879172	164208171	no known genes
6119	14	deletion	0.73	105469324	106195564	IGH@14q32.33
6119	21	gain	46.94	1	46944323	Whole chromosome gain
9534	2	gain	0.81	109749837	110563324	MALL, NPHP1
9534	9	deletion	1.20	21795269	22992317	CDKN2A, CDKN2B
9534	14	deletion	0.81	105384823	106195564	IGH@14q32.33
9534	21	gain	46.94	1	46944323	Whole chromosome gain
11538	2	deletion	2.18	88857041	91034025	IGK@2p11.2
11538	3	deletion	0.27	163941171	164208171	BC019327
11538	4	deletion	0.74	68901209	69643271	UGT2B17
11538	7	deletion	0.06	50378517	50440011	IKZF1
11538	7	deletion	0.22	141993717	142217405	TRB@7q34
11538	8	deletion	0.22	39341523	39561021	ADAM5P
11538	9	deletion	1.25	21067573	22316164	IFNA2, MTAP with a region of homozygous deletion from 21,963,069 to 21,998,595 bp involving CDKN2A and CDKN2E
11538	9	deletion	0.31	36579597	36889532	PAX5
11538	12	deletion	0.77	11634343	12405988	BCL2L14, LRP6 with homozygous deletion from 11,926,331 to 11,965,858 bp involving ETV6
11538	14	deletion	0.17	21920050	22086378	TRA@14q11.2
11538	14	deletion	1.05	88442811	89493818	FOXN3
11538	14	deletion	1.25	90275138	91525676	GPR68, SMEK1, MTAC2D1
11538	14	deletion	0.93	105384765	106311854	IGH@14q32.33
11538	21	gain	46.94	1	46944323	Whole chromosome gain
11538	22	deletion	0.22	20707319	20929851	IGL@22q11.2

7104	2	deletion	0.15	88857041	89009520	IGK@2p11.2
7104	6	deletion	0.32	26381557	26706284	Butyrophilin gene cluster within MHC regior
7104	7	deletion	0.14	38254009	38390270	TRG@7p14.1
7104	8	deletion	0.22	39341523	39561021	ADAM5P
7104	9	deletion	2.67	9725747	12395963	PTPRD
7104	9	deletion	8.51	21399799	29908742	MTAP, TEK, LINGO2, with homozygous deletion from 21,958,040 to 23,714,813 bp involving CDKN2A and CDKN2I
7104	9	deletion	3.05	34601845	37650526	DCTN3, UNC13B, RECK, PAX5, ZCCHC7, FRMPD1
7104	13	deletion	0.10	47878623	47978473	RB1
7104	14	deletion	0.45	105384765	105833371	IGH@14q32.33
7104	15	deletion	5.92	26829498	32751434	MTMR15, TRPM1, CHRNA7, RYR3, AVEN, SLC12A6
7104	22	deletion	0.14	21443734	21588228	IGL@22q11.2
7219	2	deletion	0.24	88966416	89207762	IGK@2p11.2
7219	3	deletion	1.19	60025437	61210581	FHIT
7219	6	deletion	0.27	26381557	26652292	BTN1A1, BTN2A1, BTN3A3
7219	6	deletion	0.14	32520387	32659492	HLA-DRB1
7219	7	deletion	0.14	38254009	38390270	TRG@7p14.1
7219	7	deletion	0.13	50337974	50470438	IKZF1
7219	7	deletion	0.22	141993717	142217405	TRB@7q34
7219	9	deletion	0.68	2029441	2709260	SMARCA2, VLDLR
7219	9	deletion	0.06	21963069	22026445	CDKN2A, CDKN2B
7219	9	deletion	0.31	37019089	37331059	PAX5, ZCCHC7
7219	10	deletion	7.91	127071458	134983479	BCCIP, ADAM12, DOCK1, PTPRE, MGMT, EBF3, INPP5A
7219	13	deletion	0.04	47878623	47919561	RB1
7219	14	deletion	0.28	21803298	22086378	TRA@14q11.2
7219	14	deletion	0.96	105384765	106349755	IGH@14q32.33
7219	22	deletion	0.75	20690616	21443734	IGL@22q11.2

Supplementary Table 4: Extent of deletions for *IKZF1*, *PAX5*, *CDKN2A* and *CDKN2B* in translocation and deletion samples determined by aCGH

Patient ID	Translocation or Deletion	IKZF1	PAX5	CDKN2A	CDKN2B
7243	Translocation	e3-e7	No deletion	Whole gene	Whole gene
8765	Translocation	Whole gene	No deletion	Whole gene	Whole gene
11687 (diagnostic)	Translocation	Whole gene	e1-e4	Whole gene	Majority e1-e2
11687 (relapse)	Translocation	e2-e7	e1-e5	Whole gene	Majority e1-e2
L326/05	Translocation	e3-e7	No deletion	Whole gene	Whole gene
L759/02	Translocation	No deletion	No deletion	Whole gene	e2
L1200/02	Translocation	Whole gene	Whole gene	Whole gene	Whole gene
L889/01	Translocation	e1-e7	e1	Whole gene	Whole gene
MHH-CALL-4	Translocation	e1- majority of e3	e1-e7	Whole gene	e2
MUTZ5	Translocation	e3-e7	e1-e6	Whole gene	Whole gene
4318	Deletion	e2-e6	Whole gene	Whole gene	Whole gene
6119	Deletion	No deletion	No deletion	No deletion	No deletion
9534	Deletion	No deletion	No deletion	Whole gene	Whole gene
11538	Deletion	e3-e7	e8-e10	Whole gene	Whole gene
7104	Deletion	No deletion	Whole gene	Whole gene	Whole gene
7219	Deletion	e3-e7	e1	e1	Whole gene